

SIXTH ORDER COMPACT FINITE DIFFERENCE SCHEME FOR POISSON INTERFACE PROBLEM WITH SINGULAR SOURCES

QIWEI FENG, BIN HAN AND PETER MINEV

ABSTRACT. Let Γ be a smooth curve inside a two-dimensional rectangular region Ω . In this paper, we consider the Poisson interface problem $-\nabla^2 u = f$ in $\Omega \setminus \Gamma$ with Dirichlet boundary condition such that f is smooth in $\Omega \setminus \Gamma$ and the jump functions $[u]$ and $[\nabla u \cdot \vec{n}]$ across Γ are smooth along Γ . This Poisson interface problem includes the weak solution of $-\nabla^2 u = f + g\delta_\Gamma$ in Ω as a special case. Because the source term f is possibly discontinuous across the interface curve Γ and contains a delta function singularity along the curve Γ , both the solution u of the Poisson interface problem and its flux $\nabla u \cdot \vec{n}$ are often discontinuous across the interface. To solve the Poisson interface problem with singular sources, in this paper we propose a sixth order compact finite difference scheme on uniform Cartesian grids. Our proposed compact finite difference scheme with explicitly given stencils extends the immersed interface method (IIM) to the highest possible accuracy order six for compact finite difference schemes on uniform Cartesian grids, but without the need to change coordinates into the local coordinates as in most papers on IIM in the literature. Also in contrast with most published papers on IIM, we explicitly provide the formulas for all involved stencils and therefore, our proposed scheme can be easily implemented and is of interest to practitioners dealing with Poisson interface problems. Note that the curve Γ splits Ω into two disjoint subregions Ω^+ and Ω^- . The coefficient matrix A in the resulting linear system $Ax = b$, following from the proposed scheme, is independent of any source term f , jump condition $g\delta_\Gamma$, interface curve Γ and Dirichlet boundary conditions, while only b depends on these factors and is explicitly given, according to the configuration of the nine stencil points in Ω^+ or Ω^- . The constant coefficient matrix A facilitates the parallel implementation of the algorithm in case of a large size matrix and only requires the update of the right hand side vector b for different Poisson interface problems. The scheme can be readily extended to three space dimensions as well. Due to the flexibility and explicitness of the proposed scheme, it can be generalized to obtain the highest order compact finite difference scheme for non-uniform grids as well. Our numerical experiments confirm the sixth accuracy order of the proposed compact finite difference scheme on uniform meshes for the Poisson interface problems with various singular sources.

1. INTRODUCTION AND PROBLEM FORMULATION

Interface problems are common in many practical problems such as modeling flows in composite materials, oil reservoir simulations, nuclear waste disposal, and other flows in porous media [13]. For example, in groundwater or oil reservoir modelling the permeability of the porous medium can change drastically across the interfaces between various geological layers and this can significantly affect the transport process [30]. The coefficients of heterogeneous and anisotropic diffusion problems may also be highly oscillatory, and may contain a wide range of various spatial scales, so very fine meshes are required in any standard finite difference/element discretization in order to capture the small scale features. Thus, speed and storage are two important criteria in choosing suitable algorithms for solving such problems.

High jumps in the coefficient functions can cause severe singularities in the exact solutions of the equations [2, 4, 11, 16–20, 26–29]. In general, the solutions of such problems have limited smoothness and the error analysis of their approximations by finite elements, [9], and finite differences, [31], for problems with weak solutions could be used. However, such error estimates show convergence rates that are lower than the observed in the computational practice for interface problems. Thus, an

2010 *Mathematics Subject Classification.* 65N06, 35J05, 76S05, 41A58.

Key words and phrases. Poisson interface equations, high order compact finite difference schemes, discontinuous and singular source terms, delta source functions along curves, piecewise smooth solutions.

Research supported in part by Natural Sciences and Engineering Research Council (NSERC) of Canada.

accurate tailored approximation and an error analysis which takes into account the specificity of such problem is an important and challenging task.

One possible approach to the resolution of this issue is provided by the so called immersed interface methods (IIM) proposed by LeVeque and Li (see [21,23–25] and the references therein). The main idea behind this approach is to adjust the finite difference approximation of the differential operators in the vicinity of the interface using Taylor expansions, so that the approximation order remains similar to the order of the approximation in the regions where no singularities are present, thus avoiding the need of a local grid refinement. The explicit-jump immersed interface method, introduced in [37], is based on the same idea, however, instead of modification of the discrete operators, it modifies explicitly the right hand side of the problem, and derives a second order finite difference scheme for problems with discontinuous, piecewise constant coefficients. In fact this approach is quite similar to the famous immersed boundary method (IBM) of Peskin [40]. Exploiting the idea of the IIM, in [10] the authors construct a fourth order compact finite difference method for the Helmholtz equation with discontinuous coefficients across straight vertical line interfaces. [6] derives a compact finite difference method for piecewise smooth coefficients, so that the solution and its gradient can both achieve a second order of accuracy. [7] considers anisotropic elliptic interface problems whose coefficient matrix is symmetric semi-positive definite and derives a hybrid discretization involving finite elements away of the interfaces, and an immersed interface finite difference approximation near or at the interfaces. The error in the maximum norm is order $O(h^2 \log \frac{1}{h})$. In addition to the treatment of interface problems, Taylor expansions can be used to derive high order compact finite difference schemes for regular elliptic problems. A family of fourth and sixth order compact finite difference methods for the three-dimensional Poisson equation are derived in [38]. [32] concludes that the highest order for a compact finite difference method for the two-dimensional Poisson's equation on uniform grids is sixth.

Another source of singularity in the solution of elliptic problems is the presence of singularities in the source term. One possible regularization of Dirac delta functions is analyzed in [33], and [39] introduces the high order matched interface and boundary (MIB) method for elliptic equations with singular sources. Similarly, the finite difference discretization of such problems are considered by [34]. In [3] the idea of the IBM is combined with a Discontinuous Galerkin (DG) spatial discretization to derive a high-order method for elliptic problems with discontinuous coefficients and singular sources. In [14], the authors combine the idea of the IIM with a continuous finite element discretization to derive a high order finite element method for elliptic problems with jumps in the solution and its flux across smooth interfaces. Elliptic problems with point-located Dirac delta source terms are considered in [8]. A second order approximation to the singular source is combined with a second order finite difference approximation of the operator on Cartesian grids with hanging nodes, that allow for local refinements around the singular points. Another finite difference version of the immersed interface method is used to solve the heat diffusion with singular sources in [15].

Singular solutions, induced by discontinuous coefficients of singular sources can also be approximated using a continuous finite element approximation, by enriching the basis with singular functions located in the proper spatial locations, as considered in [1,4,11,12,17,19,20]. Alternatively, a posteriori error estimates can be used to devise grid refinement algorithms, as demonstrated for example in [29], where such estimates are provided in case of interface problems with discontinuous coefficients.

This short literature review is far from being complete, however, one can conclude that there are not many available discretizations of elliptic problems with singularities, that can achieve higher-than-second order of accuracy, and not rely on a local grid refinement. It is particularly challenging to derive a compact finite difference scheme that can achieve the highest possible order of accuracy i.e. a compact scheme of order six. The derivation of such a scheme is the main goal of the present paper. In particular, we consider Poisson's equations with discontinuous or singular source terms, such that the solution and the normal component of gradient can be discontinuous across an interface curve.

To fix the ideas, let $\Omega = (l_1, l_2) \times (l_3, l_4)$ be a two-dimensional rectangular region. Let also ψ be a smooth two-dimensional function and consider a smooth curve $\Gamma := \{(x, y) \in \Omega : \psi(x, y) = 0\}$, which partitions Ω into two subregions: $\Omega^+ := \{(x, y) \in \Omega : \psi(x, y) > 0\}$ and $\Omega^- := \{(x, y) \in \Omega : \psi(x, y) < 0\}$. We define $f_{\pm} := f\chi_{\Omega_{\pm}}$ and $u_{\pm} := u\chi_{\Omega_{\pm}}$. The particular examples for $\psi(x, y) = x^2 + y^2 - 2$ and $\psi(x, y) = y - \cos(x)$ are illustrated in Fig. 1. We now state the Poisson interface

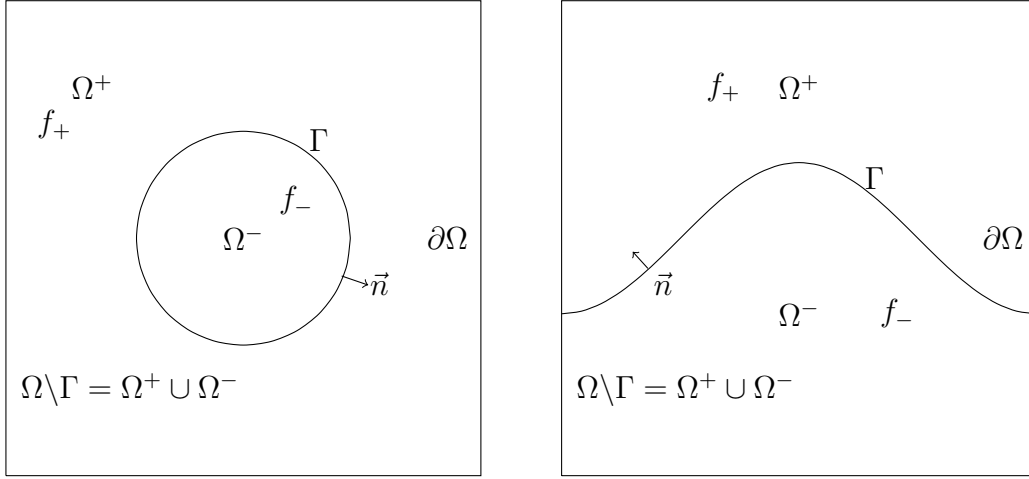


FIGURE 1. The problem region $\Omega = (-\pi, \pi)^2$ and the two subregions $\Omega^+ = \{(x, y) \in \Omega : \psi(x, y) > 0\}$ and $\Omega^- = \{(x, y) \in \Omega : \psi(x, y) < 0\}$ partitioned by the interface curve $\Gamma = \{(x, y) \in \Omega : \psi(x, y) = 0\}$ with the functions $\psi(x, y) = x^2 + y^2 - 2$ (left) and $\psi(x, y) = y - \cos(x)$ (right). Note that $\Omega \setminus \Gamma = \Omega^+ \cup \Omega^-$.

problem with singular sources as follows:

$$\begin{cases} -\nabla^2 u = f & \text{in } \Omega \setminus \Gamma, \\ u = g_0 & \text{on } \partial\Omega, \\ [u] = g_1 & \text{on } \Gamma, \\ [\nabla u \cdot \vec{n}] = g & \text{on } \Gamma, \end{cases} \quad (1.1)$$

which, if $g_1 = 0$, can be equivalently rewritten as

$$\begin{cases} -\nabla^2 u = f - g\delta_{\Gamma} & \text{in } \Omega, \\ u = g_0 & \text{on } \partial\Omega. \end{cases} \quad (1.2)$$

Here \vec{n} is the unit normal vector of Γ pointing towards Ω^+ , and for a point $(x_0, y_0) \in \Gamma$,

$$[u](x_0, y_0) := \lim_{(x,y) \in \Omega^+, (x,y) \rightarrow (x_0, y_0)} u(x, y) - \lim_{(x,y) \in \Omega^-, (x,y) \rightarrow (x_0, y_0)} u(x, y), \quad (1.3)$$

$$[\nabla u \cdot \vec{n}](x_0, y_0) := \lim_{(x,y) \in \Omega^+, (x,y) \rightarrow (x_0, y_0)} \nabla u(x, y) \cdot \vec{n} - \lim_{(x,y) \in \Omega^-, (x,y) \rightarrow (x_0, y_0)} \nabla u(x, y) \cdot \vec{n}. \quad (1.4)$$

The conditions in (1.3) and (1.4) are called jump conditions for interface problems.

The Poisson interface problem in (1.1) with singular sources arise in many applications. In chemical reaction-diffusion processes, the solution u represents the chemical concentration [5, 15]. In case of catalytic reactions the catalyst is usually distributed in a very thin layer over an interface Γ , and therefore the reaction can be considered as occurring on a $d - 1$ -dimensional manifold in a d -dimensional space. Such reactions result in a continuous chemical concentration u , but a discontinuous gradient ∇u across the interface Γ , i.e., $g_1(x, y) = 0$ and $g(x, y) \neq 0$ for all $(x, y) \in \Gamma$.

Problems with discontinuous solutions and/or discontinuous fluxes appear also in multicomponent incompressible flows with or without interfacial tension. As discussed by [22], if surface tension is present at the interface the incompressibility constraint, applied to the momentum equation yields a pressure Poisson equation with a dipole source (the gradient of the delta function representing the interfacial tension alongside the fluid-fluid interface). Since such a source function is difficult to

approximate, its effect can be modeled via interface jump conditions for the pressure and its gradient. The solution for the velocity is always continuous across the interface, however, If the viscosities of the fluids on both sides of the interface differ, its flux has a jump there. So, both the velocity and the pressure can be subject to elliptic problems with jumps of the solution or its flux across fluid-fluid or fluid-elastic-structure interfaces.

Similar jumps appear in the solution for the pressure u and velocity \vec{v} , of the set of the Darcy's and continuity equations:

$$\vec{v} = -\frac{k}{\mu}\nabla u, \quad (1.5)$$

$$\nabla \cdot \vec{v} = f, \quad (1.6)$$

in case of a discontinuous mobility $\frac{k}{\mu}$ and/or singular source f :

In this paper we consider the Poisson interface problem in (1.1) under the following assumptions:

- f is smooth in each of Ω^+ and Ω^- , and f may be discontinuous across the interface curve Γ .
- All functions ψ , g , g_0 and g_1 are smooth.
- The exact solution u is piecewise smooth in the sense that u has uniformly continuous partial derivatives of (total) order up to seven in each of the subregions Ω^+ and Ω^- .

The remainder of the paper is organized as follows. In Section 2, we derive the sixth order compact finite difference scheme at regular and irregular points, and discuss their consistency in Theorem 2.2. and Theorem 2.4, correspondingly. Here the center of a stencil is called a regular point if it, together with all other eight points in the stencil are completely inside Ω^+ or are completely outside Ω^+ . Otherwise, it is called an irregular point. We also give a simple proof for the maximum order of compact schemes at regular points. In Theorem 2.3 we provide an expression for the jump of certain derivatives of the solution, due to the interface conditions. In 2D there are 72 different configurations for the stencil, depending on how the interface curve partitions the nine points in it. Up to a symmetry and rigid motion, all configurations at an irregular point can be classified into nine typical cases, see Figs. 3 to 5 for a graphical representation of these configurations. In Section 3, we provide numerical experiments to check the convergence rate measured in l_2 and l_∞ norms. We test the numerical examples in four cases: (1) the exact solution is known and Γ does not intersect $\partial\Omega$; (2) the exact solution is known and Γ intersects $\partial\Omega$; (3) the exact solution is unknown and Γ does not intersect $\partial\Omega$; and (4) the exact solution is unknown and Γ intersects $\partial\Omega$. In Section 4, we summarize the main contributions of this paper. Finally, in Appendix A we shall provide the detailed proof for Theorem 2.3, which plays a key role in our development of the compact stencils at irregular points in Section 2.

2. STENCILS FOR SIXTH ORDER COMPACT FINITE DIFFERENCE SCHEMES USING UNIFORM CARTESIAN GRIDS

Recall that the problem domain is $\Omega = (l_1, l_2) \times (l_3, l_4)$. Because we shall use uniform Cartesian meshes, we require that the longer side of Ω is a multiple of the shorter side of Ω . Without loss of generality, we can assume $l_4 - l_3 = N_0(l_2 - l_1)$ for some positive integer N_0 . For any positive integer $N_1 \in \mathcal{N}$, we define $N_2 := N_0 N_1$ and then the grid size is $h := (l_2 - l_1)/N_1 = (l_4 - l_3)/N_2$.

Let $x_i = l_1 + ih$ and $y_j = l_3 + jh$ for $i = 1, \dots, N_1 - 1$ and $j = 1, \dots, N_2 - 1$. Because in this paper we are only interested in compact finite difference schemes on uniform Cartesian grids, for a compact stencil centered at the center point (x_i, y_j) , the compact stencil involves nine points $(x_i + kh, y_j + lh)$ for $k, l \in \{-1, 0, 1\}$. It is convenient to use a level set function ψ , which is a two-dimensional smooth function, to describe a given smooth interface curve Γ through

$$\Gamma := \{(x, y) \in \Omega : \psi(x, y) = 0\}.$$

Then the interface curve Γ splits the problem domain Ω into two subregions: $\Omega^+ := \{(x, y) \in \Omega : \psi(x, y) > 0\}$ and $\Omega^- := \{(x, y) \in \Omega : \psi(x, y) < 0\}$. Now the interface curve Γ splits these nine points into two groups depending on whether these points lie inside Ω^+ or Ω^- . If a grid point lies on

the curve Γ , then the grid point lies on the boundaries of both Ω^+ and Ω^- . For simplicity we may assume that the grid point belongs to Ω^+ and we can use the interface conditions to handle such a grid point. Therefore, we naturally define

$$d_{i,j}^+ := \{(k, \ell) : k, \ell \in \{-1, 0, 1\}, \psi(x_i + kh, y_j + \ell h) \geq 0\}$$

and

$$d_{i,j}^- := \{(k, \ell) : k, \ell \in \{-1, 0, 1\}, \psi(x_i + kh, y_j + \ell h) < 0\}.$$

That is, the interface curve Γ splits the nine points in a compact stencil into two disjoint sets $\{(x_{i+k}, y_{j+\ell}) : (k, \ell) \in d_{i,j}^+\} \subseteq \Omega^+$ and $\{(x_{i+k}, y_{j+\ell}) : (k, \ell) \in d_{i,j}^-\} \subseteq \Omega^-$. We say that a grid/center point (x_i, y_j) is a *regular point* if $d_{i,j}^+ = \emptyset$ or $d_{i,j}^- = \emptyset$. That is, the center point (x_i, y_j) of a stencil is regular if all its nine points are completely inside Ω^+ (hence $d_{i,j}^- = \emptyset$) or inside Ω^- (i.e., $d_{i,j}^+ = \emptyset$). See Fig. 2 for an example of regular points. Otherwise, the center point (x_i, y_j) of a stencil is called an *irregular point* if $d_{i,j}^+ \neq \emptyset$ and $d_{i,j}^- \neq \emptyset$. That is, the interface curve Γ splits the nine points into two disjoint nonempty sets. As explained before, up to a symmetry and rigid motion, all the compact stencils at an irregular point can be classified into nine typical cases, see Figs. 3 to 5 for these nine typical cases.

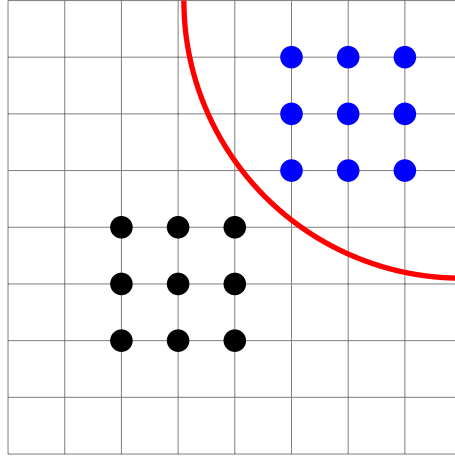


FIGURE 2. An example of regular points. The curve in red color is the interface curve Γ .

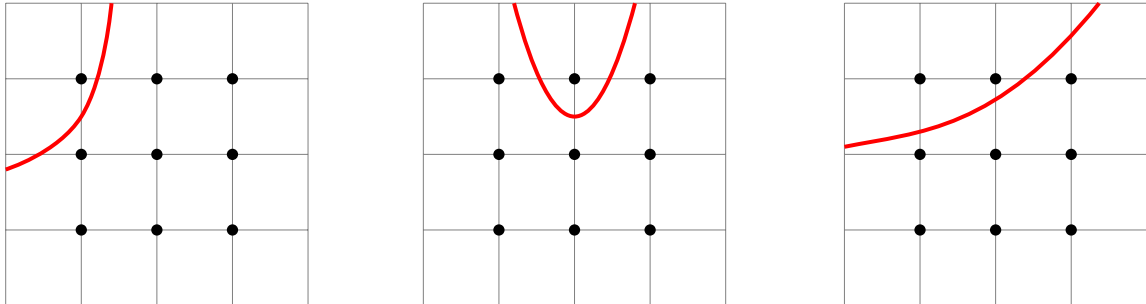


FIGURE 3. Examples for irregular points. The curve in red color is the interface curve Γ .

Let M be a positive integer standing for a given desired accuracy order. Before we discuss the compact schemes at a regular or an irregular point (x_i, y_j) , let us introduce some notations and then outline the main ideas for finding the stencils at a general grid point (x_i, y_j) , achieving a given accuracy order M .

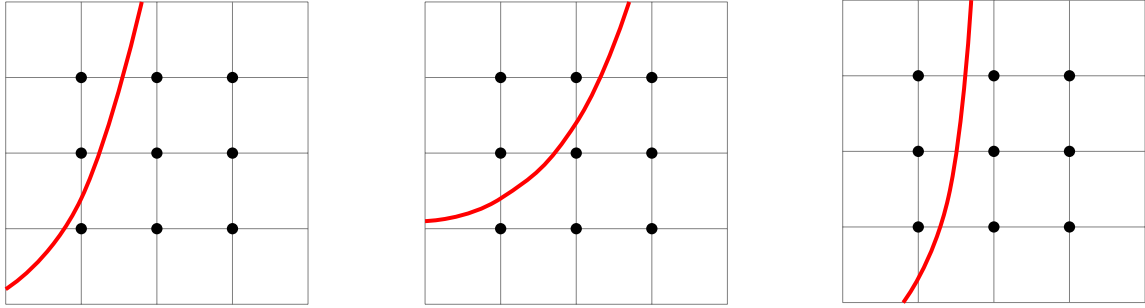


FIGURE 4. Examples for irregular points. The curve in red color is the interface curve Γ .

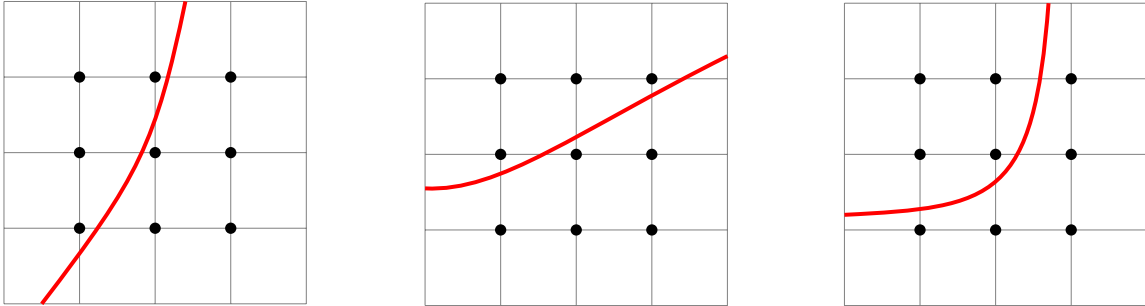


FIGURE 5. Examples for irregular points. The curve in red color is the interface curve Γ .

We first pick up and fix a base point (x_i^*, y_j^*) inside the open square $(x_i - h, x_i + h) \times (y_j - h, y_j + h)$. That is, we can write

$$x_i^* = x_i - v_0 \quad \text{and} \quad y_j^* = y_j - w_0 \quad \text{with} \quad -h < v_0, w_0 < h. \quad (2.1)$$

For the sake of brevity, we shall use the following notions:

$$u^{(m,n)} := \frac{\partial^{m+n} u}{\partial^m x \partial^n y}(x_i^*, y_j^*) \quad \text{and} \quad f^{(m,n)} := \frac{\partial^{m+n} f}{\partial^m x \partial^n y}(x_i^*, y_j^*), \quad (2.2)$$

which are just their (m, n) th partial derivatives at the base point (x_i^*, y_j^*) . Define $\mathbb{N}_0 := \mathbb{N} \cup \{0\}$, the set of all nonnegative integers. For a nonnegative integer $K \in \mathbb{N}_0$, we define

$$\Lambda_K := \{(m, n - m) : n = 0, \dots, K \text{ and } m = 0, \dots, n\}, \quad K \in \mathbb{N}_0. \quad (2.3)$$

For a smooth function u , its values $u(x + x_i^*, y + y_j^*)$ for small x, y can be well approximated through its Taylor polynomial below:

$$u(x + x_i^*, y + y_j^*) = \sum_{(m,n) \in \Lambda_{M+1}} \frac{u^{(m,n)}}{m!n!} x^m y^n + \mathcal{O}(h^{M+2}), \quad x, y \in (-2h, 2h). \quad (2.4)$$

In other words, in a neighborhood of the base point (x_i^*, y_j^*) , the function u is well approximated and completely determined by the partial derivatives of u of total degree less than $M + 2$ at the base point (x_i^*, y_j^*) , i.e., by the unknown quantities $u^{(m,n)}$, $(m, n) \in \Lambda_{M+1}$. We can similarly approximate $f(x + x_i^*, y + y_j^*)$ for small x, y . For $x \in \mathbb{R}$, the floor function $\lfloor x \rfloor$ is defined to be the largest integer less than or equal to x . For an integer m , we define

$$\text{odd}(m) := \begin{cases} 0, & \text{if } m \text{ is even,} \\ 1, & \text{if } m \text{ is odd.} \end{cases}$$

That is, $\text{odd}(m) = m - 2\lfloor m/2 \rfloor$ and $\lfloor m/2 \rfloor = \frac{m - \text{odd}(m)}{2}$. Because the function u is a solution to the partial differential equation in (1.1), we shall see that all the quantities $u^{(m,n)}$, $(m, n) \in \Lambda_{M+1}$ are not independent of each other. In fact, we have:

Lemma 2.1. *Let u be a function satisfying $-\nabla^2 u = f$ in $\Omega \setminus \Gamma$. If a point $(x_i^*, y_j^*) \in \Omega \setminus \Gamma$, then*

$$u^{(m,n)} = (-1)^{\lfloor \frac{m}{2} \rfloor} u^{(\text{odd}(m), n+m-\text{odd}(m))} + \sum_{\ell=1}^{\lfloor m/2 \rfloor} (-1)^\ell f^{(m-2\ell, n+2\ell-2)}, \quad \forall (m, n) \in \Lambda_{M+1}^2, \quad (2.5)$$

where the subsets Λ_{M+1}^1 and Λ_{M+1}^2 of Λ_{M+1} are defined by

$$\Lambda_{M+1}^2 := \Lambda_{M+1} \setminus \Lambda_{M+1}^1 \quad \text{with} \quad \Lambda_{M+1}^1 := \{(\ell, k - \ell) : k = \ell, \dots, M + 1 - \ell \text{ and } \ell = 0, 1\}. \quad (2.6)$$

Proof. By our assumption, we have $u_{xx} + u_{yy} = -f$ in $\Omega \setminus \Gamma$. Therefore, we obtain

$$u^{(m+2,n)} + u^{(m,n+2)} = -f^{(m,n)}, \quad \forall m, n \in \mathbb{N}_0. \quad (2.7)$$

Hence, for $(m, n) \in \Lambda_{M+1}^2$, we have $m \geq 2$ and

$$u^{(m,n)} = -f^{(m-2,n)} - u^{(m-2,n+2)}, \quad (m, n) \in \Lambda_{M+1}^2.$$

Then we can recursively apply the above identity $\frac{m - \text{odd}(m)}{2} - 1$ times to get (2.5). \square

For the convenience of the reader, see Fig. 6 for an illustration of the quantities $u^{(m,n)}$, $(m, n) \in \Lambda_{M+1}^1$ and $(m, n) \in \Lambda_{M+1}^2$ in Lemma 2.1 with $M = 6$.

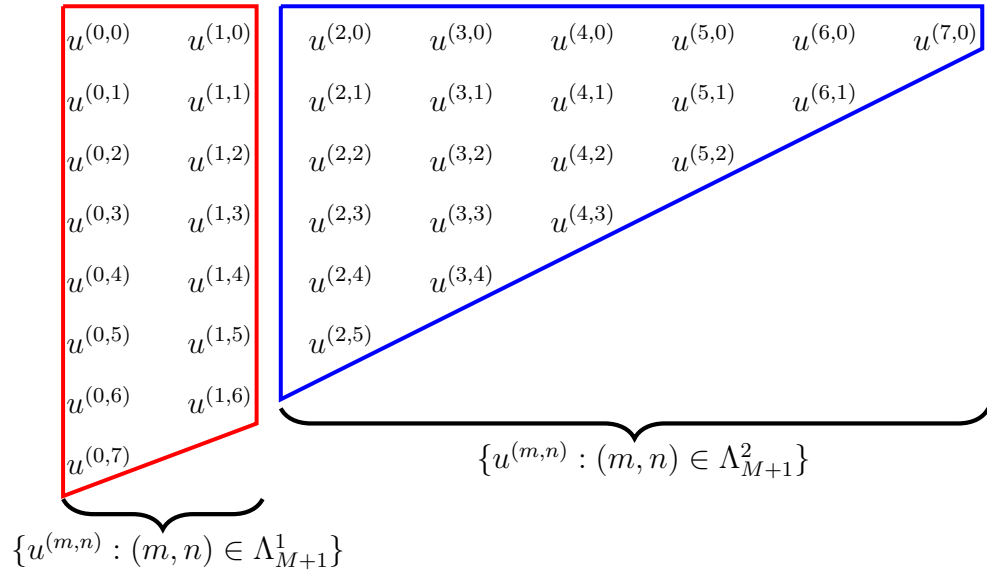


FIGURE 6. Red trapezoid: $\{u^{(m,n)} : (m, n) \in \Lambda_{M+1}^1\}$ with $M = 6$. Blue trapezoid: $\{u^{(m,n)} : (m, n) \in \Lambda_{M+1}^2\}$ with $M = 6$. Note that $\Lambda_{M+1} = \Lambda_{M+1}^1 \cup \Lambda_{M+1}^2$.

For $M = 6$, the identities in (2.5) of Lemma 2.1 for $u^{(m,n)}$, $(m, n) \in \Lambda_7^2$ can be explicitly given by

$$\begin{aligned} u^{(2,1)} &= -f^{(0,1)} - u^{(0,3)}, & u^{(2,2)} &= -f^{(0,2)} - u^{(0,4)}, & u^{(2,3)} &= -f^{(0,3)} - u^{(0,5)}, & u^{(2,4)} &= -f^{(0,4)} - u^{(0,6)}, \\ u^{(2,5)} &= -f^{(0,5)} - u^{(0,7)}, & u^{(3,0)} &= -f^{(1,0)} - u^{(1,2)}, & u^{(3,1)} &= -f^{(1,1)} - u^{(1,3)}, & u^{(3,2)} &= -f^{(1,2)} - u^{(1,4)}, \\ u^{(3,3)} &= -f^{(1,3)} - u^{(1,5)}, & u^{(3,4)} &= -f^{(1,4)} - u^{(1,6)}, & u^{(4,0)} &= -f^{(2,0)} + f^{(0,2)} + u^{(0,4)}, \\ u^{(4,1)} &= -f^{(2,1)} + f^{(0,3)} + u^{(0,5)}, & u^{(4,2)} &= -f^{(2,2)} + f^{(0,4)} + u^{(0,6)}, & u^{(4,3)} &= -f^{(2,3)} + f^{(0,5)} + u^{(0,7)}, \\ u^{(5,0)} &= -f^{(3,0)} + f^{(1,2)} + u^{(1,4)}, & u^{(5,1)} &= -f^{(3,1)} + f^{(1,3)} + u^{(1,5)}, & u^{(5,2)} &= -f^{(3,2)} + f^{(1,4)} + u^{(1,6)}, \\ u^{(6,0)} &= -f^{(4,0)} + f^{(2,2)} - f^{(0,4)} - u^{(0,6)}, & u^{(6,1)} &= -f^{(4,1)} + f^{(2,3)} - f^{(0,5)} - u^{(0,7)}, \\ u^{(7,0)} &= -f^{(5,0)} + f^{(3,2)} - f^{(1,4)} - u^{(1,6)}. \end{aligned} \quad (2.8)$$

Note that the cardinality of Λ_{M+1} equals the sum of the cardinalities of Λ_{M+1}^1 and Λ_{M-1} . The identities in (2.5) of Lemma 2.1 show that every $u^{(m,n)}, (m,n) \in \Lambda_{M+1}$ can be written as a linear combination of the quantities $u^{(m,n)}, (m,n) \in \Lambda_{M+1}^1$ and $f^{(m,n)}, (m,n) \in \Lambda_{M-1}$. Conversely, by (2.7), every $f^{(m,n)}, (m,n) \in \Lambda_{M-1}$ and every $u^{(m,n)}, (m,n) \in \Lambda_{M+1}^1$ can be trivially written as linear combinations of $u^{(m,n)} \in \Lambda_{M+1}$. Because the source term f is known, this can reduce the number of constraints on $u^{(m,n)}, (m,n) \in \Lambda_{M+1}$ for the function u satisfying (1.1). Now using (2.5), we can rewrite the approximation of $u(x + x_i^*, y + y_j^*)$ in (2.4) as follows:

$$\begin{aligned} \sum_{(m,n) \in \Lambda_{M+1}} \frac{u^{(m,n)}}{m!n!} x^m y^n &= \sum_{(m,n) \in \Lambda_{M+1}^1} \frac{u^{(m,n)}}{m!n!} x^m y^n + \sum_{(m,n) \in \Lambda_{M+1}^2} \frac{u^{(m,n)}}{m!n!} x^m y^n \\ &= \sum_{(m,n) \in \Lambda_{M+1}^1} u^{(m,n)} G_{m,n}(x, y) + \sum_{(m,n) \in \Lambda_{M-1}} f^{(m,n)} H_{m,n}(x, y), \end{aligned}$$

where $G_{m,n}$ and $H_{m,n}$ are polynomials uniquely determined by the identities in (2.5). Explicitly,

$$G_{m,n}(x, y) := \sum_{\ell=0}^{\lfloor \frac{n}{2} \rfloor} (-1)^\ell \frac{x^{m+2\ell} y^{n-2\ell}}{(m+2\ell)!(n-2\ell)!}, \quad m \in \{0, 1\}, n \in \mathbb{N}_0 \quad (2.9)$$

and

$$H_{m,n}(x, y) := \sum_{\ell=1-\lfloor \frac{m}{2} \rfloor}^{1+\lfloor \frac{n}{2} \rfloor} \frac{(-1)^\ell x^{m+2\ell} y^{n-2\ell+2}}{(m+2\ell)!(n-2\ell+2)!}, \quad m, n \in \mathbb{N}_0. \quad (2.10)$$

From (2.5) we observe that $G_{m,n}$ is a homogeneous polynomial of total degree $m+n$ for all $(m,n) \in \Lambda_{M+1}^1$, while $H_{m,n}$ is a homogeneous polynomial of total degree $m+n+2$ for all $(m,n) \in \Lambda_{M-1}$. For $M=6$, all the polynomials $G_{m,n}, (m,n) \in \Lambda_7^1$ and $H_{m,n}, (m,n) \in \Lambda_5$ are explicitly given by

$$\begin{aligned} G_{0,0} &= 1, \quad G_{0,1} = y, \quad G_{0,2} = \frac{1}{2}y^2 - \frac{1}{2}x^2, \quad G_{0,3} = \frac{1}{6}y^3 - \frac{1}{2}x^2y, \quad G_{0,4} = \frac{1}{24}y^4 + \frac{1}{24}x^4 - \frac{1}{4}x^2y^2, \\ G_{0,5} &= \frac{1}{120}y^5 - \frac{1}{12}x^2y^3 + \frac{1}{24}x^4y, \quad G_{0,6} = \frac{1}{720}y^6 - \frac{1}{720}x^6 - \frac{1}{48}x^2y^4 + \frac{1}{48}x^4y^2, \\ G_{0,7} &= \frac{1}{5040}y^7 + \frac{1}{144}x^4y^3 - \frac{1}{720}x^6y - \frac{1}{240}x^2y^5, \quad G_{1,0} = x, \quad G_{1,1} = xy, \quad G_{1,2} = \frac{1}{2}xy^2 - \frac{1}{6}x^3, \\ G_{1,3} &= \frac{1}{6}xy^3 - \frac{1}{6}x^3y, \quad G_{1,4} = \frac{1}{24}xy^4 + \frac{1}{120}x^5 - \frac{1}{12}x^3y^2, \quad G_{1,5} = \frac{1}{120}xy^5 - \frac{1}{36}x^3y^3 + \frac{1}{120}x^5y, \\ G_{1,6} &= \frac{1}{720}xy^6 - \frac{1}{5040}x^7 + \frac{1}{240}x^5y^2 - \frac{1}{144}x^3y^4, \end{aligned} \quad (2.11)$$

and

$$\begin{aligned} H_{0,0} &= -\frac{1}{2}x^2, \quad H_{0,1} = -\frac{1}{2}x^2y, \quad H_{0,2} = \frac{1}{24}x^4 - \frac{1}{4}x^2y^2, \quad H_{0,3} = -\frac{1}{12}x^2y^3 + \frac{1}{24}x^4y, \\ H_{0,4} &= -\frac{1}{720}x^6 - \frac{1}{48}x^2y^4 + \frac{1}{48}x^4y^2, \quad H_{0,5} = \frac{1}{144}x^4y^3 - \frac{1}{720}x^6y - \frac{1}{240}x^2y^5, \quad H_{1,0} = -\frac{1}{6}x^3, \quad H_{1,1} = -\frac{1}{6}x^3y, \\ H_{1,2} &= \frac{1}{120}x^5 - \frac{1}{12}x^3y^2, \quad H_{1,3} = \frac{1}{120}x^5y - \frac{1}{36}x^3y^3, \quad H_{1,4} = -\frac{1}{5040}x^7 + \frac{1}{240}x^5y^2 - \frac{1}{144}x^3y^4, \quad H_{2,0} = -\frac{1}{24}x^4, \\ H_{2,1} &= -\frac{1}{24}x^4y, \quad H_{2,2} = \frac{1}{720}x^6 - \frac{1}{48}x^4y^2, \quad H_{2,3} = -\frac{1}{144}x^4y^3 + \frac{1}{720}x^6y, \quad H_{3,0} = -\frac{1}{120}x^5, \\ H_{3,1} &= -\frac{1}{120}x^5y, \quad H_{3,2} = \frac{1}{5040}x^7 - \frac{1}{240}x^5y^2, \quad H_{4,0} = -\frac{1}{720}x^6, \quad H_{4,1} = -\frac{1}{720}x^6y, \quad H_{5,0} = -\frac{1}{5040}x^7. \end{aligned} \quad (2.12)$$

Hence, by (2.4), the solution u to (1.1) near the base point (x_i^*, y_j^*) can be approximated by

$$u(x + x_i^*, y + y_j^*) = \sum_{(m,n) \in \Lambda_{M+1}^1} u^{(m,n)} G_{m,n}(x, y) + \sum_{(m,n) \in \Lambda_{M-1}} f^{(m,n)} H_{m,n}(x, y) + \mathcal{O}(h^{M+2}), \quad (2.13)$$

for $x, y \in (-2h, 2h)$. We shall use the above identity in (2.13) for finding compact stencils achieving a desired accuracy order M .

2.1. Regular points. In this subsection, we discuss how to find a compact scheme centered at a regular point (x_i, y_j) , which has been well studied in the literature. The main purpose of this subsection is to outline the main ideas. For simplicity, we just pick (x_i, y_j) as the base point (x_i^*, y_j^*) , that is, (x_i^*, y_j^*) is defined in (2.1) with $v_0 = w_0 = 0$. Recall that $M \in \mathbb{N}$ stands for the desired

accuracy order. For a compact stencil at a regular point (x_i, y_j) , we need to find stencil coefficients $\{C_{k,\ell}\}_{k,\ell=-1,0,1}$ and $\{C_{f,m,n}\}_{(m,n)\in\Lambda_{M-1}}$ satisfying

$$\sum_{k=-1}^1 \sum_{\ell=-1}^1 C_{k,\ell}(h)u(x_i + kh, y_j + \ell h) = \sum_{(m,n)\in\Lambda_{M-1}} f^{(m,n)}C_{f,m,n}(h) + \mathcal{O}(h^{M+2}), \quad h \rightarrow 0, \quad (2.14)$$

where $C_{k,\ell}$ and $C_{f,m,n}$ are to-be-determined polynomials of h with degree less than $M + 2$. Plugging the approximation in (2.13) into the above stencil in (2.14) to approximate $u(x_i + kh, y_j + \ell h)$, the conditions in (2.14) become

$$\sum_{(m,n)\in\Lambda_{M+1}^1} u^{(m,n)}I_{m,n}(h) + \sum_{(m,n)\in\Lambda_{M-1}} f^{(m,n)}(J_{m,n}(h) - C_{f,m,n}(h)) = \mathcal{O}(h^{M+2}), \quad (2.15)$$

where

$$I_{m,n}(h) := \sum_{k=-1}^1 \sum_{\ell=-1}^1 C_{k,\ell}(h)G_{m,n}(kh, \ell h), \quad J_{m,n}(h) := \sum_{k=-1}^1 \sum_{\ell=-1}^1 C_{k,\ell}(h)H_{m,n}(kh, \ell h). \quad (2.16)$$

Since (2.15) must hold for all unknowns $u^{(m,n)}$, $(m,n) \in \Lambda_{M+1}^1$ and $f^{(m,n)}$, $(m,n) \in \Lambda_{M-1}$, to find nontrivial stencil coefficients $C_{k,\ell}(h)$ for $k, \ell = -1, 0, 1$, solving (2.15) is equivalent to solving

$$I_{m,n}(h) = \mathcal{O}(h^{M+2}) \quad h \rightarrow 0, \quad \text{for all } (m,n) \in \Lambda_{M+1}^1 \quad (2.17)$$

and

$$J_{m,n}(h) = C_{f,m,n}(h) + \mathcal{O}(h^{M+2}), \quad h \rightarrow 0, \quad \text{for all } (m,n) \in \Lambda_{M-1}. \quad (2.18)$$

Note that the solutions of $\{C_{k,\ell}\}_{k,\ell=-1,0,1}$ and $\{C_{f,m,n}\}_{(m,n)\in\Lambda_{M-1}}$ to (2.17) and (2.18) are homogeneous in terms of its unknowns, that is, a solution multiplied with a given polynomial of h to all coefficients is still a solution. Hence, we say that a solution for the coefficients in a compact stencil is nontrivial if $C_{k,\ell}(0) \neq 0$ for at least some $k, \ell = -1, 0, 1$. Since $G_{m,n}$ is a homogeneous polynomial of degree $m + n$, we can write $G_{m,n}(kh, \ell h) = g_{m,n,k,\ell}h^{m+n}$ for some constants $g_{m,n,k,\ell}$. Hence, (2.17) becomes

$$\sum_{k=-1}^1 \sum_{\ell=-1}^1 C_{k,\ell}(h)g_{m,n,k,\ell} = \mathcal{O}(h^{M+2-m-n}), \quad h \rightarrow 0, \quad \text{for all } (m,n) \in \Lambda_{M+1}^1. \quad (2.19)$$

Because $M + 2 - m - n \geq 1$ for all $(m,n) \in \Lambda_{M+1}^1$, the identities in (2.19) automatically imply

$$\sum_{k=-1}^1 \sum_{\ell=-1}^1 C_{k,\ell}(0)g_{m,n,k,\ell} = 0, \quad \text{for all } (m,n) \in \Lambda_{M+1}^1. \quad (2.20)$$

By calculation, the maximum integer M for the linear system in (2.20) to have a nontrivial solution $\{C_{k,\ell}(0)\}_{k,\ell=-1,0,1}$ is $M = 6$. More precisely, the rank of the matrix $(g_{m,n,k,\ell})_{(m,n)\in\Lambda_{M+1}^1, (k,\ell)\in\{-1,0,1\}^2}$ is nine for $M = 7$ (hence (2.20) has only the trivial solution for $M = 7$) and its rank is 8 for $M = 6$. Therefore, for a compact stencil, the maximum accuracy order M that we can achieve is $M = 6$. Moreover, up to a multiplicative constant, such a nontrivial solution $\{C_{k,\ell}(0)\}_{k,\ell=-1,0,1}$ to (2.20) is uniquely given by

$$C_{0,0} = -20, \quad C_{-1,0} = C_{1,0} = C_{0,-1} = C_{0,1} = 4, \quad C_{-1,-1} = C_{-1,1} = C_{1,-1} = C_{1,1} = 1. \quad (2.21)$$

For a constant solution of $\{C_{k,\ell}(0)\}_{k,\ell=-1,0,1}$ satisfying (2.20), such a constant solution obviously satisfies also (2.19) and therefore, it is a nontrivial solution to (2.17).

Since $H_{m,n}$ is a homogeneous polynomial of degree $m + n + 2$, we can write $H_{m,n}(kh, \ell h) = h_{m,n,k,\ell}h^{m+n+2}$ for some constants $h_{m,n,k,\ell}$. Now plugging (2.21) into the definition of $J_{m,n}$, we easily deduce from (2.18) that all the coefficients $C_{f,m,n}$ satisfying (2.18) are given by

$$C_{f,m,n}(h) := \sum_{k=-1}^1 \sum_{\ell=-1}^1 C_{k,\ell}H_{m,n}(h) = \sum_{k=-1}^1 \sum_{\ell=-1}^1 C_{k,\ell}h_{m,n,k,\ell}h^{m+n+2}, \quad (m,n) \in \Lambda_5. \quad (2.22)$$

Explicitly,

$$C_{f,0,0} := -6h^2, \quad C_{f,0,2} = C_{f,2,0} := -\frac{1}{2}h^4, \quad C_{f,0,4} = C_{f,4,0} := -\frac{1}{60}h^6, \quad C_{f,2,2} := -\frac{1}{15}h^6$$

and all other coefficients $C_{f,m,n}(h) = 0$. In summary, for a regular point (x_i, y_j) , we obtain the following theorem which is well known in the literature (e.g., see [32, 36, 38]).

Theorem 2.2. *Let a grid point (x_i, y_j) be a regular point, i.e., either $d_{i,j}^+ = \emptyset$ or $d_{i,j}^- = \emptyset$. Let $(u_h)_{i,j}$ be the numerical approximated solution of the exact solution u of the partial differential equation (1.1) at a regular point (x_i, y_j) . Then the scheme:*

$$(u_h)_{i-1,j-1} + 4(u_h)_{i-1,j} + (u_h)_{i-1,j+1} + 4(u_h)_{i,j-1} - 20(u_h)_{i,j} + 4(u_h)_{i,j+1} + (u_h)_{i+1,j-1} + 4(u_h)_{i+1,j} + (u_h)_{i+1,j+1} = -6h^2 f^{(0,0)} - \frac{1}{2}h^4(f^{(0,2)} + f^{(2,0)}) - \frac{1}{60}h^6(f^{(0,4)} + f^{(4,0)}) - \frac{1}{15}h^6 f^{(2,2)}, \quad (2.23)$$

achieves sixth order accuracy for $-\nabla^2 u = f$, where $f^{(m,n)} := \frac{\partial^{m+n} f}{\partial^m x \partial^n y}(x_i, y_j)$. Moreover,

- (i) The compact finite difference scheme of order four can be obtained from (2.23) by dropping the terms $\frac{1}{60}h^6(f^{(0,4)} + f^{(4,0)})$ and $\frac{1}{15}h^6 f^{(2,2)}$.
- (ii) The maximum accuracy order M for a compact finite difference scheme is $M = 6$.

2.2. Irregular points. Let (x_i, y_j) be an irregular point, that is, both $d_{i,j}^P \neq \emptyset$ and $d_{i,j}^N \neq \emptyset$. In this subsection, we shall find a compact stencil at an irregular point (x_i, y_j) for a given accuracy order M . The idea is essentially the same, although the technicalities are much more complicated.

Let (x_i, y_j) be an irregular point and we shall take a base point $(x_i^*, y_j^*) \in \Gamma \cap (x_i - h, x_i + h) \times (y_j - h, y_j + h)$ on the interface Γ and inside $(x_i - h, x_i + h) \times (y_j - h, y_j + h)$. That is, as in (2.1),

$$x_i^* = x_i - v_0 \quad \text{and} \quad y_j^* = y_j - w_0 \quad \text{with} \quad -h < v_0, w_0 < h \quad \text{and} \quad (x_i^*, y_j^*) \in \Gamma. \quad (2.24)$$

Let u_{\pm} and f_{\pm} represent the solution u and source term f in Ω^+ or Ω^- , respectively. As in (2.2), we define

$$u_{\pm}^{(m,n)} := \frac{\partial^{m+n} u_{\pm}}{\partial^m x \partial^n y}(x_i^*, y_j^*), \quad f_{\pm}^{(m,n)} := \frac{\partial^{m+n} f_{\pm}}{\partial^m x \partial^n y}(x_i^*, y_j^*)$$

and

$$g^{(m,n)} := \frac{\partial^{m+n} g}{\partial^m x \partial^n y}(x_i^*, y_j^*), \quad g_1^{(m,n)} := \frac{\partial^{m+n} g_1}{\partial^m x \partial^n y}(x_i^*, y_j^*).$$

Since the base point (x_i^*, y_j^*) is now on the interface Γ , the equation $-\nabla^2 u = f$ is no longer valid at the base point (x_i^*, y_j^*) . However, the curve Γ is smooth and we assumed that the solution u and f are piecewise smooth. More precisely, u_+ and f_+ on Ω^+ can be extended into smooth functions in a neighborhood of (x_i^*, y_j^*) , while u_- and f_- on Ω^- can be extended into smooth functions in a neighborhood of (x_i^*, y_j^*) . Therefore, Lemma 2.1 still holds for u_{\pm} and f_{\pm} . In other words, the identities in (2.5) hold by replacing u and f by u_{\pm} and f_{\pm} , respectively. Consequently, the key identity in (2.13) still holds by replacing u and f with u_{\pm} and f_{\pm} , respectively. Explicitly,

$$u_{\pm}(x + x_i^*, y + y_j^*) = \sum_{(m,n) \in \Lambda_{M+1}^1} u_{\pm}^{(m,n)} G_{m,n}(x, y) + \sum_{(m,n) \in \Lambda_{M-1}} f_{\pm}^{(m,n)} H_{m,n}(x, y) + \mathcal{O}(h^{M+2}), \quad (2.25)$$

for $x, y \in (-2h, 2h)$, where the index sets Λ_{M+1}^1 and Λ_{M-1} are defined in (2.6) and (2.3), respectively, while the polynomials $G_{m,n}(x, y)$ and $H_{m,n}(x, y)$ are defined in (2.9) and (2.10), respectively.

For a compact stencil at an irregular point (x_i, y_j) to achieve a given accuracy order M , we need to find nontrivial stencil coefficients satisfying

$$\begin{aligned} \sum_{k=-1}^1 \sum_{\ell=-1}^1 C_{k,\ell}(h) u(x_i + kh, y_j + \ell h) &= \sum_{(m,n) \in \Lambda_{M-1}} C_{f_+,m,n}(h) f_+^{(m,n)} + \sum_{(m,n) \in \Lambda_{M-1}} C_{f_-,m,n}(h) f_-^{(m,n)} \\ &+ \sum_{(m,n) \in \Lambda_{M+1}} C_{g_1,m,n}(h) g_1^{(m,n)} + \sum_{(m,n) \in \Lambda_M} C_{g,m,n}(h) g^{(m,n)} + \mathcal{O}(h^{M+2}), \quad h \rightarrow 0, \end{aligned} \quad (2.26)$$

where $C_{k,\ell}, C_{f_{\pm},m,n}, C_{g_1,m,n}$ and $C_{g,m,n}$ are to-be-determined polynomials of h having degree less than $M + 2$. Because some indices (k, ℓ) may come from $d_{i,j}^+$ while others from $d_{i,j}^-$, we need to link information on Ω^+ and Ω^- at the base point $(x_i^*, y_j^*) \in \Gamma$. To do so, instead of using the level set function ψ to describe the interface curve Γ , we shall now assume that we have a parametric equation for Γ near the base point (x_i^*, y_j^*) . We can easily obtain such a parametric equation by locally solving $\psi(x, y) = 0$ near the base point (x_i^*, y_j^*) for either x or y . That is, it suffices to consider one of the following two simple parametric representations of Γ :

$$x = t + x_i^*, \quad y = r(t) + y_j^* \quad \text{or} \quad x = r(t) + x_i^*, \quad y = t + y_j^*, \quad \text{for } t \in (-\epsilon, \epsilon) \quad \text{with } \epsilon > 0, \quad (2.27)$$

for a smooth function r , since Γ is assumed to be smooth. Note that the parameter corresponding to the base point (x_i^*, y_j^*) is $t = 0$ with $r(0) = 0$. It is important to notice that we do not need to actually solve $\psi(x, y) = 0$ to get the function r , because we only need the derivatives of $r(t)$ at $t = 0$, which can be easily obtained from $\psi(x, y) = 0$ through the Implicit Function Theorem. To cover the above two cases of parametric equations in (2.27) for Γ together, we discuss the following general parametric equation for Γ :

$$x = r(t) + x_i^*, \quad y = s(t) + y_j^*, \quad (r'(t))^2 + (s'(t))^2 > 0 \quad \text{for } t \in (-\epsilon, \epsilon) \quad \text{with } \epsilon > 0. \quad (2.28)$$

Note that the parameter t for the base point (x_i^*, y_j^*) is $t = 0$ and it is also important to notice that $r(0) = s(0) = 0$.

Using the interface conditions in (1.1), we now link the two sets $\{u_-^{(m,n)} : (m, n) \in \Lambda_{M+1}^1\}$ and $\{u_+^{(m,n)} : (m, n) \in \Lambda_{M+1}^1\}$ through the following result, whose proof is given in Appendix A.

Theorem 2.3. *Let u be the solution to the Poisson interface problem in (1.1) and the base point $(x_i^*, y_j^*) \in \Gamma$, which is parameterized near (x_i^*, y_j^*) by (2.28). Then*

$$\begin{aligned} u_-^{(m',n')} &= u_+^{(m',n')} + \sum_{(m,n) \in \Lambda_{M-1}} \left(T_{m',n',m,n}^+ f_+^{(m,n)} + T_{m',n',m,n}^- f_-^{(m,n)} \right) \\ &+ \sum_{(m,n) \in \Lambda_{M+1}} T_{m',n',m,n}^{g_1} g_1^{(m,n)} + \sum_{(m,n) \in \Lambda_M} T_{m',n',m,n}^g g^{(m,n)}, \quad \forall (m', n') \in \Lambda_{M+1}^1, \end{aligned} \quad (2.29)$$

where all the transmission coefficients T^{\pm}, T^{g_1}, T^g are uniquely determined by $r^{(k)}(0)$ and $s^{(k)}(0)$ for $k = 0, \dots, M + 1$ and can be easily obtained by recursively calculating $U^{(m',n')} := u_+^{(m',n')} - u_-^{(m',n')}$, $(m', n') \in \Lambda_{M+1}^1$ through the recursive formulas given in (A.7) and (A.29).

Now we discuss how to find a compact stencil at an irregular point (x_i, y_j) with the given accuracy order M . Since the set $\{-1, 0, 1\}^2$ is the disjoint union of $d_{i,j}^+$ and $d_{i,j}^-$, we can write

$$\begin{aligned} &\sum_{k=-1}^1 \sum_{\ell=-1}^1 C_{k,\ell}(h) u(x_i + kh, y_j + \ell h) \\ &= \sum_{(k,\ell) \in d_{i,j}^+} C_{k,\ell}(h) u(x_i^* + v_0 + kh, y_j^* + w_0 + \ell h) + \sum_{(k,\ell) \in d_{i,j}^-} C_{k,\ell}(h) u(x_i^* + v_0 + kh, y_j^* + w_0 + \ell h). \end{aligned}$$

Using (2.25), we have

$$\sum_{(k,\ell) \in d_{i,j}^{\pm}} C_{k,\ell}(h) u(x_i^* + v_0 + kh, y_j^* + w_0 + \ell h) = \sum_{(m,n) \in \Lambda_{M+1}^1} u_{\pm}^{(m,n)} I_{m,n}^{\pm}(h) + \sum_{(m,n) \in \Lambda_{M-1}} f_{\pm}^{(m,n)} J_{m,n}^{\pm,0}(h), \quad (2.30)$$

where

$$I_{m,n}^{\pm}(h) := \sum_{(k,\ell) \in d_{i,j}^{\pm}} C_{k,\ell}(h) G_{m,n}(v_0 + kh, w_0 + \ell h), \quad J_{m,n}^{\pm,0}(h) := \sum_{(k,\ell) \in d_{i,j}^{\pm}} C_{k,\ell}(h) H_{m,n}(v_0 + kh, w_0 + \ell h).$$

Now using the transmission coefficients in Theorem 2.3, we have

$$\begin{aligned} \sum_{(m',n') \in \Lambda_{M+1}^1} u_{-}^{(m',n')} I_{m',n'}^{-}(h) &= \sum_{(m',n') \in \Lambda_{M+1}^1} u_{+}^{(m',n')} I_{m',n'}^{-}(h) + \sum_{(m,n) \in \Lambda_{M-1}} \left(f_{+}^{(m,n)} J_{m,n}^{+,T}(h) + f_{-}^{(m,n)} J_{m,n}^{-,T}(h) \right) \\ &+ \sum_{(m,n) \in \Lambda_{M+1}} g_1^{(m,n)} J_{m,n}^{g_1}(h) + \sum_{(m,n) \in \Lambda_M} g^{(m,n)} J_{m,n}^g(h), \end{aligned}$$

where

$$\begin{aligned} J_{m,n}^{\pm,T}(h) &:= \sum_{(m',n') \in \Lambda_{M+1}^1} I_{m',n'}^{-}(h) T_{m',n',m,n}^{\pm}, \\ J_{m,n}^{g_1}(h) &:= \sum_{(m',n') \in \Lambda_{M+1}^1} I_{m',n'}^{-}(h) T_{m',n',m,n}^{g_1}, \quad J_{m,n}^g(h) := \sum_{(m',n') \in \Lambda_{M+1}^1} I_{m',n'}^{-}(h) T_{m',n',m,n}^g. \end{aligned} \quad (2.31)$$

Putting everything together we have

$$\begin{aligned} \sum_{k=-1}^1 \sum_{\ell=-1}^1 C_{k,\ell}(h) u(x_i + kh, y_j + \ell h) &= \sum_{(m,n) \in \Lambda_{M+1}^1} u_{+}^{(m,n)} I_{m,n}(h) + \sum_{(m,n) \in \Lambda_{M-1}} f_{+}^{(m,n)} J_{m,n}^{+}(h) \\ &+ \sum_{(m,n) \in \Lambda_{M-1}} f_{-}^{(m,n)} J_{m,n}^{-}(h) + \sum_{(m,n) \in \Lambda_{M+1}} g_1^{(m,n)} J_{m,n}^{g_1}(h) + \sum_{(m,n) \in \Lambda_M} g^{(m,n)} J_{m,n}^g(h), \end{aligned} \quad (2.32)$$

where

$$I_{m,n}(h) := I_{m,n}^{+}(h) + I_{(m,n)}^{-}(h), \quad J_{m,n}^{\pm}(h) := J_{m,n}^{\pm,0}(h) + J_{m,n}^{\pm,T}(h). \quad (2.33)$$

Note that all the unknowns are $u_{+}^{(m,n)}$ for $(m,n) \in \Lambda_{M+1}^1$, $f_{\pm}^{(m,n)}$ for $(m,n) \in \Lambda_{M-1}$, $g_1^{(m,n)}$ for $(m,n) \in \Lambda_{M+1}$ and $g^{(m,n)}$ for $(m,n) \in \Lambda_M$. Therefore, to find a compact stencil at an irregular point (x_i, y_j) with a desired accuracy order M , the conditions in (2.26) are equivalent to

$$I_{m,n}(h) = \mathcal{O}(h^{M+2}), \quad h \rightarrow 0, \quad \text{for all } (m,n) \in \Lambda_{M+1}^1, \quad (2.34)$$

$$J_{m,n}^{\pm}(h) = C_{f_{\pm},m,n}(h) + \mathcal{O}(h^{M+2}), \quad h \rightarrow 0, \quad \text{for all } (m,n) \in \Lambda_{M-1}, \quad (2.35)$$

$$J_{m,n}^{g_1}(h) = C_{g_1,m,n}(h) + \mathcal{O}(h^{M+2}), \quad h \rightarrow 0, \quad \text{for all } (m,n) \in \Lambda_{M+1}, \quad (2.36)$$

$$J_{m,n}^g(h) = C_{g,m,n}(h) + \mathcal{O}(h^{M+2}), \quad h \rightarrow 0, \quad \text{for all } (m,n) \in \Lambda_M. \quad (2.37)$$

Due to the relations in (2.29) of Theorem 2.3, we observe that the solution $\{C_{k,\ell}\}_{k,\ell=-1,0,1}$ in (2.21) is also a solution to (2.34) with $M = 6$. Now similar to (2.22), plugging the values of $\{C_{k,\ell}\}_{k,\ell=-1,0,1}$ in (2.21) into (2.35), (2.36) and (2.37) with $M = 6$, we obtain all the other stencil coefficients given by

$$C_{f_{\pm},m,n}(h) := J_{m,n}^{\pm}(h), \quad (m,n) \in \Lambda_5, \quad (2.38)$$

$$C_{g_1,m,n}(h) := J_{m,n}^{g_1}(h), \quad (m,n) \in \Lambda_7 \quad \text{and} \quad C_{g,m,n}(h) = J_{m,n}^g(h), \quad (m,n) \in \Lambda_6. \quad (2.39)$$

In summary, we obtain the following theorem for compact stencils at irregular points.

Theorem 2.4. *Let $(u_h)_{i,j}$ be the numerical solution of (1.1) at an irregular point (x_i, y_j) . Pick a base point (x_i^*, y_j^*) as in (2.24). Then the following compact scheme centered at the irregular point (x_i, y_j) :*

$$\begin{aligned} (u_h)_{i-1,j-1} + 4(u_h)_{i-1,j} + (u_h)_{i-1,j+1} + 4(u_h)_{i,j-1} - 20(u_h)_{i,j} + 4(u_h)_{i,j+1} + (u_h)_{i+1,j-1} \\ + 4(u_h)_{i+1,j} + (u_h)_{i+1,j+1} &= \sum_{(m,n) \in \Lambda_5} f_{+}^{(m,n)} J_{m,n}^{+}(h) + \sum_{(m,n) \in \Lambda_5} f_{-}^{(m,n)} J_{m,n}^{-}(h) \\ &+ \sum_{(m,n) \in \Lambda_7} g_1^{(m,n)} J_{m,n}^{g_1}(h) + \sum_{(m,n) \in \Lambda_6} g^{(m,n)} J_{m,n}^g(h), \end{aligned} \quad (2.40)$$

achieves sixth order of accuracy, where the quantities $J_{m,n}^{\pm}(m,n) \in \Lambda_5$, $J_{m,n}^{g_1}(m,n) \in \Lambda_7$ and $J_{m,n}^g(m,n) \in \Lambda_6$ are given in (2.33) and (2.31), respectively. Moreover, the stencils for the accuracy order $M = 3, 4, 5$ can be easily obtained from the stencil in (2.40) by dropping $G_{m,n}$ with $m + n > M + 1$ and $H_{m,n}$ with $m + n > M - 1$.

3. NUMERICAL EXPERIMENTS

Let $\Omega = (l_1, l_2) \times (l_3, l_4)$ with $l_4 - l_3 = N_0(l_2 - l_1)$ for some positive integer N_0 . For a given $J \in \mathbb{N}_0$, we define $h := (l_2 - l_1)/N_1$ with $N_1 := 2^J$ and let $x_i = l_1 + ih$ and $y_j = l_3 + jh$ for $i = 1, 2, \dots, N_1 - 1$ and $j = 1, 2, \dots, N_2 - 1$ with $N_2 := N_0 N_1$. Let $u(x, y)$ be the exact solution of (1.1) and $(u_h)_{i,j}$ be the numerical solution at (x_i, y_j) using the mesh size h . We shall measure the consistency of our proposed scheme in the l_2 norm by the relative error $\frac{\|u_h - u\|_2}{\|u\|_2}$ if the exact solution u is available, and by the relative error $\frac{\|u_h - u_{h/2}\|_2}{\|u_{h/2}\|_2}$ if the exact solution is not known (and hence we use the next level numerical solution $u_{h/2}$ as a reference solution), where

$$\begin{aligned} \|u_h - u\|_2^2 &:= \frac{1}{N} \sum_{i=1}^{N_1-1} \sum_{j=1}^{N_2-1} ((u_h)_{i,j} - u(x_i, y_j))^2, & \|u\|_2^2 &:= \frac{1}{N} \sum_{i=1}^{N_1-1} \sum_{j=1}^{N_2-1} (u(x_i, y_j))^2, \\ \|u_h - u_{h/2}\|_2^2 &:= \frac{1}{N} \sum_{i=1}^{N_1-1} \sum_{j=1}^{N_2-1} ((u_h)_{i,j} - (u_{h/2})_{2i,2j})^2, & \|u_{h/2}\|_2^2 &:= \frac{1}{N} \sum_{i=1}^{N_1-1} \sum_{j=1}^{N_2-1} ((u_{h/2})_{2i,2j})^2, \end{aligned}$$

where $N := (N_1 - 1)(N_2 - 1)$. The errors can be also measured in the l_∞ norm as follows:

$$\|u_h - u\|_\infty := \max_{1 \leq i < N_1, 1 \leq j < N_2} |(u_h)_{i,j} - u(x_i, y_j)|, \quad \|u_h - u_{h/2}\|_\infty := \max_{1 \leq i < N_1, 1 \leq j < N_2} |(u_h)_{i,j} - (u_{h/2})_{2i,2j}|.$$

In addition, κ denotes the condition number of the coefficient matrix. According to Theorems 2.2 and 2.4, (1.1) has the same coefficient matrix. So we only provide the values of κ in Table 1.

3.1. Numerical examples with u known and $\Gamma \cap \partial\Omega = \emptyset$. In this subsection, we provide a few numerical experiments such that the exact solution u of (1.1) is known and the interface curve Γ does not touch the boundary of Ω .

Example 1. Let $\Omega = (-\pi, \pi)^2$ and the interface curve be given by $\Gamma := \{(x, y) \in \Omega : \psi(x, y) = 0\}$ with $\psi(x, y) = x^2 + y^2 - 2$. Note that $\Gamma \cap \partial\Omega = \emptyset$ and the exact solution u of (1.1) is given by

$$u_+ = u\chi_{\Omega^+} = \sin(4x)(2 - (x^2 + y^2))^2, \quad u_- = u\chi_{\Omega^-} = \cos(4y)(2 - (x^2 + y^2))^2 + 100.$$

All the functions f, g, g_0, g_1 in (1.1) can be obtained by plugging the above exact solution into (1.1). In particular, $g_1 = -100$ and $g = 0$. The numerical results are presented in Table 1 and Fig. 7.

TABLE 1. Performance in Example 1 of the proposed sixth order compact finite difference scheme in Theorems 2.2 and 2.4 on uniform Cartesian meshes with $h = 2^{-J} \times 2\pi$. κ is the condition number of the coefficient matrix.

J	$\frac{\ u_h - u\ _2}{\ u\ _2}$	order	$\ u_h - u\ _\infty$	order	$\frac{\ u_h - u_{h/2}\ _2}{\ u_{h/2}\ _2}$	order	$\ u_h - u_{h/2}\ _\infty$	order	κ
3	3.65E+00	0	3.55E+02	0	3.08E+00	0	3.40E+02	0	3.14E+01
4	1.25E-01	4.868	1.90E+01	4.224	1.24E-01	4.631	1.89E+01	4.165	1.26E+02
5	6.60E-04	7.566	1.03E-01	7.529	6.56E-04	7.565	1.03E-01	7.528	5.03E+02
6	3.38E-06	7.610	5.87E-04	7.456	3.35E-06	7.613	5.83E-04	7.459	2.01E+03
7	2.55E-08	7.048	4.27E-06	7.103	2.53E-08	7.050	4.24E-06	7.104	8.05E+03
8	2.40E-10	6.733	3.50E-08	6.928	3.58E-10	6.142	8.04E-08	5.720	3.22E+04

Example 2. Let $\Omega = (-\pi, \pi)^2$ and the interface curve be given by $\Gamma := \{(x, y) \in \Omega : \psi(x, y) = 0\}$ with $\psi(x, y) = \frac{y^2}{2} + \frac{x^2}{1+x^2} - \frac{1}{2}$. Note that $\Gamma \cap \partial\Omega = \emptyset$ and the exact solution u of (1.1) is given by

$$u_+ = u\chi_{\Omega^+} = \sin(2x), \quad u_- = u\chi_{\Omega^-} = \sin(2x) + 3.$$

All the functions f, g, g_0, g_1 in (1.1) can be obtained by plugging the above exact solution into (1.1). In particular, $g_1 = -3$ and $g = 0$. The numerical results are provided in Table 2 and Fig. 7.

TABLE 2. Performance in Example 2 of the proposed sixth order compact finite difference scheme in Theorems 2.2 and 2.4 on uniform Cartesian meshes with $h = 2^{-J} \times 2\pi$.

J	$\frac{\ u_h - u\ _2}{\ u\ _2}$	order	$\ u_h - u\ _\infty$	order	$\frac{\ u_h - u_{h/2}\ _2}{\ u_{h/2}\ _2}$	order	$\ u_h - u_{h/2}\ _\infty$	order
3	2.51E-02	0	7.00E-02	0	2.49E-02	0	6.96E-02	0
4	1.92E-04	7.033	6.63E-04	6.721	1.90E-04	7.036	6.59E-04	6.722
5	1.88E-06	6.667	7.48E-06	6.471	1.87E-06	6.667	7.42E-06	6.474
6	1.67E-08	6.817	6.65E-08	6.813	1.66E-08	6.814	6.60E-08	6.811
7	1.21E-10	7.112	4.94E-10	7.074	1.20E-10	7.113	4.90E-10	7.074
8	1.02E-12	6.891	4.36E-12	6.822	1.10E-12	6.769	5.06E-12	6.598

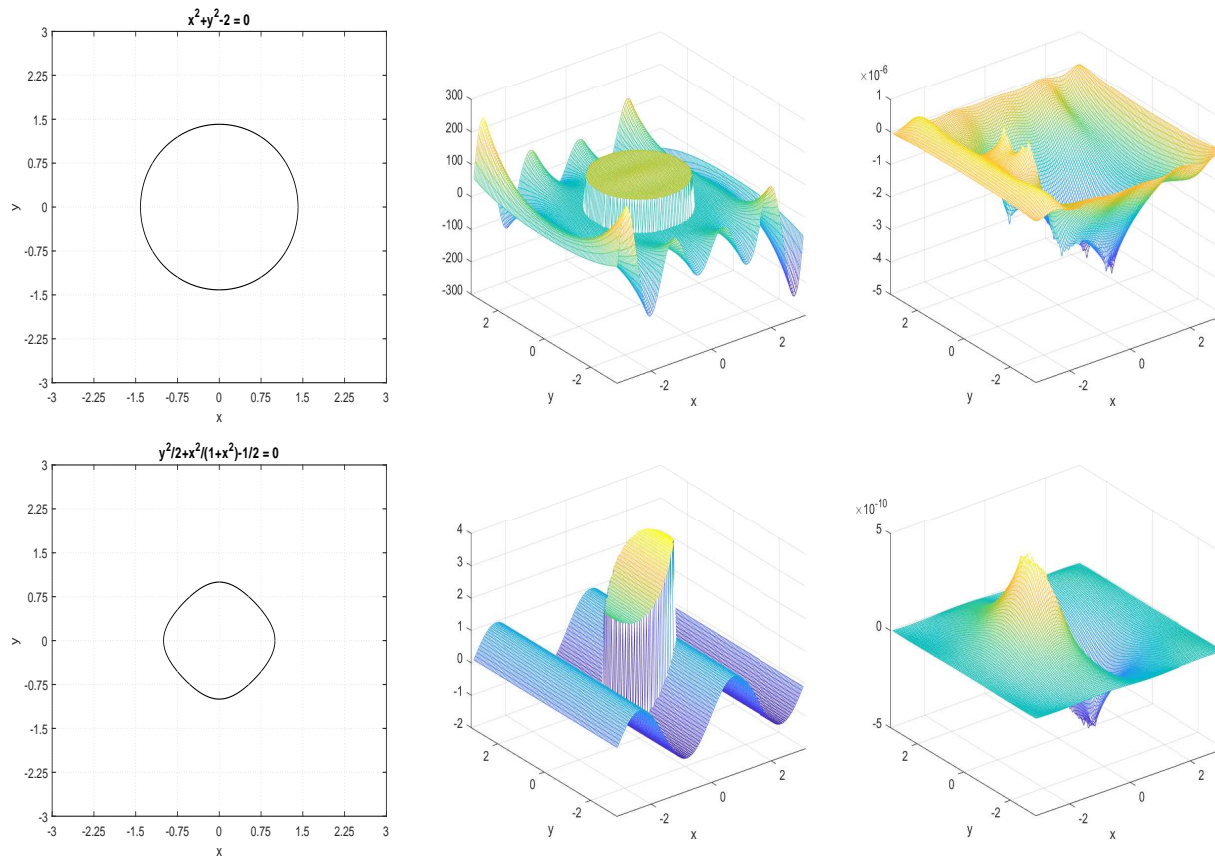


FIGURE 7. Top row for Example 1: the interface curve Γ (left), the numerical solution u_h (middle) and the error $u - u_h$ (right) with $h = 2^{-7} \times 2\pi$. Bottom row for Example 2: the interface curve Γ (left), the numerical solution u_h (middle) and the error $u - u_h$ (right) with $h = 2^{-7} \times 2\pi$.

3.2. Numerical examples with u known and $\Gamma \cap \partial\Omega \neq \emptyset$. In this subsection, we provide a few numerical experiments such that the exact solution u of (1.1) is known and the interface curve Γ touches the boundary of Ω .

Example 3. Let $\Omega = (-\frac{3}{2}\pi, \frac{3}{2}\pi)^2$ and the interface curve be given by $\Gamma := \{(x, y) \in \Omega : \psi(x, y) = 0\}$ with $\psi(x, y) = y - \cos(x)$. Note that $\Gamma \cap \partial\Omega \neq \emptyset$ and the exact solution u of (1.1) is given by

$$u_+ = u\chi_{\Omega^+} = -\sin(x)(y - \cos(x))^2, \quad u_- = u\chi_{\Omega^-} = -\cos(y)(y - \cos(x))^2 - 10.$$

All the associated functions f, g, g_0, g_1 can be obtained by plugging the above exact solution into (1.1). In particular, $g_1 = 10$ and $g = 0$. The numerical results are provided in Table 3 and Fig. 8.

TABLE 3. Performance in Example 3 of the proposed sixth order compact finite difference scheme in Theorems 2.2 and 2.4 on uniform Cartesian meshes with $h = 2^{-J} \times 3\pi$.

J	$\frac{\ u_h - u\ _2}{\ u\ _2}$	order	$\ u_h - u\ _\infty$	order	$\frac{\ u_h - u_{h/2}\ _2}{\ u_{h/2}\ _2}$	order	$\ u_h - u_{h/2}\ _\infty$	order
3	1.72E-01	0	3.28E+00	0	1.68E-01	0	3.22E+00	0
4	3.78E-03	5.508	7.36E-02	5.476	3.77E-03	5.483	7.34E-02	5.454
5	1.28E-05	8.206	2.46E-04	8.224	1.26E-05	8.224	2.42E-04	8.244
6	1.97E-07	6.024	4.25E-06	5.856	1.96E-07	6.009	4.23E-06	5.839
7	1.03E-09	7.577	2.19E-08	7.603	1.02E-09	7.586	2.16E-08	7.611
8	1.17E-11	6.462	2.68E-10	6.348	1.26E-11	6.341	2.81E-10	6.265

Example 4. Let $\Omega = (0, 3)^2$ and the interface curve be given by $\Gamma := \{(x, y) \in \Omega : \psi(x, y) = 0\}$ with $\psi(x, y) = x^2/2 + y^2/2 - 2$. Note that $\Gamma \cap \partial\Omega \neq \emptyset$ and the exact solution u of (1.1) is given by

$$u_+ = u\chi_{\Omega^+} = \sin(\pi x), \quad u_- = u\chi_{\Omega^-} = \sin(\pi x) + 2.$$

All the associated functions f, g, g_0, g_1 can be obtained by plugging the above exact solution into (1.1). In particular, $g_1 = -2$ and $g = 0$. The numerical results are provided in Table 4 and Fig. 8.

TABLE 4. Performance in Example 4 of the proposed sixth order compact finite difference scheme in Theorems 2.2 and 2.4 on uniform Cartesian meshes with $h = 2^{-J} \times 3$.

J	$\frac{\ u_h - u\ _2}{\ u\ _2}$	order	$\ u_h - u\ _\infty$	order	$\frac{\ u_h - u_{h/2}\ _2}{\ u_{h/2}\ _2}$	order	$\ u_h - u_{h/2}\ _\infty$	order
3	2.96E-03	0	1.02E-02	0	2.93E-03	0	1.02E-02	0
4	2.93E-05	6.655	1.27E-04	6.333	2.91E-05	6.652	1.26E-04	6.336
5	2.16E-07	7.086	1.03E-06	6.938	2.14E-07	7.086	1.02E-06	6.940
6	1.66E-09	7.025	8.25E-09	6.967	1.65E-09	7.025	8.19E-09	6.968
7	1.28E-11	7.013	6.70E-11	6.943	1.30E-11	6.989	6.71E-11	6.931
8	2.65E-13	5.598	9.91E-13	6.080	9.54E-13	3.763	3.06E-12	4.454

3.3. Numerical examples with u unknown and $\Gamma \cap \partial\Omega = \emptyset$. In this subsection, we provide a few numerical experiments such that the exact solution u of (1.1) is unknown and the interface curve Γ does not touch the boundary of Ω .

Example 5. Let $\Omega = (-\pi, \pi)^2$ and the interface curve be given by $\Gamma := \{(x, y) \in \Omega : \psi(x, y) = 0\}$ with $\psi(x, y) = \frac{x^2}{2} + \frac{y^2}{2} - 1$. Note that $\Gamma \cap \partial\Omega = \emptyset$ and the coefficients of (1.1) are given by

$$\begin{aligned} f_+ &= f\chi_{\Omega^+} = \sin(3x)\sin(3y), & f_- &= f\chi_{\Omega^-} = \cos(3x)\cos(3y), \\ g_0 &= 0, & g_1 &= -\exp(x-y)\sin(x+y), & g &= -\exp(x+y)\cos(x-y). \end{aligned}$$

The numerical results are provided in Table 5 and Fig. 9.

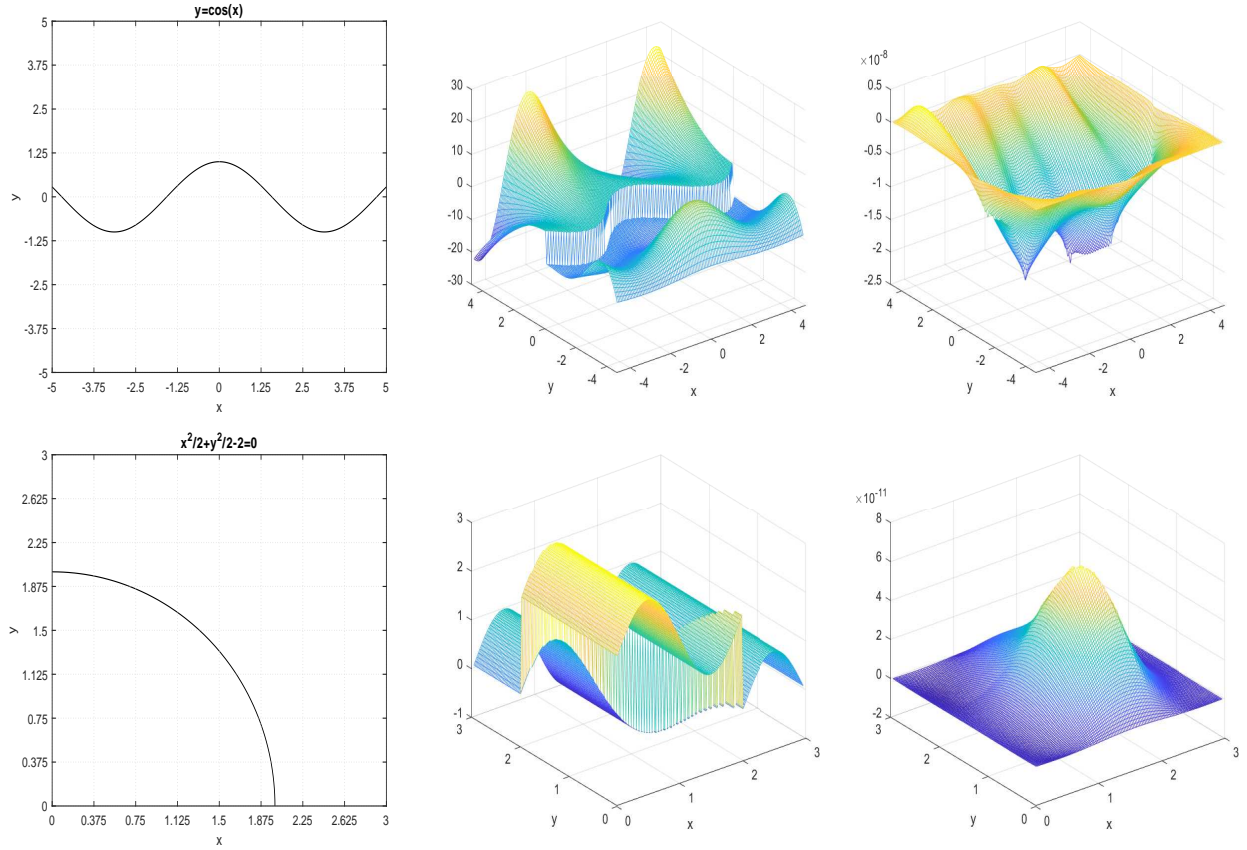


FIGURE 8. Top row for Example 3: the interface curve Γ (left), the numerical solution u_h (middle) and the error $u - u_h$ (right) with $h = 2^{-7} \times 3\pi$. Bottom row for Example 4: the interface curve Γ (left), the numerical solution u_h (middle) and the error $u - u_h$ (right) with $h = 2^{-7} \times 3$.

Example 6. Let $\Omega = (-\pi, \pi)^2$ and the interface curve be given by $\Gamma := \{(x, y) \in \Omega : \psi(x, y) = 0\}$ with $\psi(x, y) = \frac{y^2}{2} + \frac{x^2}{1+x^2} - \frac{1}{2}$. Note that $\Gamma \cap \partial\Omega = \emptyset$ and the coefficients of (1.1) are given by

$$\begin{aligned} f_+ &= f\chi_{\Omega^+} = \sin(3x)\sin(2y), & f_- &= f\chi_{\Omega^-} = \cos(2x)\cos(2y), \\ g_0 &= 0, & g_1 &= -\sin(x)\sin(y), & g &= -\cos(x)\sin(y). \end{aligned}$$

The numerical results are provided in Table 5 and Fig. 9.

TABLE 5. Performance in Example 5 and Example 6 of the proposed sixth order compact finite difference scheme in Theorems 2.2 and 2.4 on uniform Cartesian meshes with the same mesh size $h = 2^{-J} \times 2\pi$.

J	Example 5				Example 6			
	$\frac{\ u_h - u_{h/2}\ _2}{\ u_{h/2}\ _2}$	order	$\ u_h - u_{h/2}\ _\infty$	order	$\frac{\ u_h - u_{h/2}\ _2}{\ u_{h/2}\ _2}$	order	$\ u_h - u_{h/2}\ _\infty$	order
3	4.42E-01	0	1.48E+00	0	5.26E+02	0	4.01E+02	0
4	4.67E-02	3.245	9.76E-02	3.919	6.79E-02	12.919	6.00E-02	12.705
5	5.01E-04	6.541	1.01E-03	6.589	8.20E-04	6.372	9.18E-04	6.032
6	4.34E-06	6.850	1.01E-05	6.647	1.31E-05	5.974	1.44E-05	5.992
7	5.95E-08	6.190	4.52E-07	4.483	2.09E-07	5.967	2.61E-07	5.789

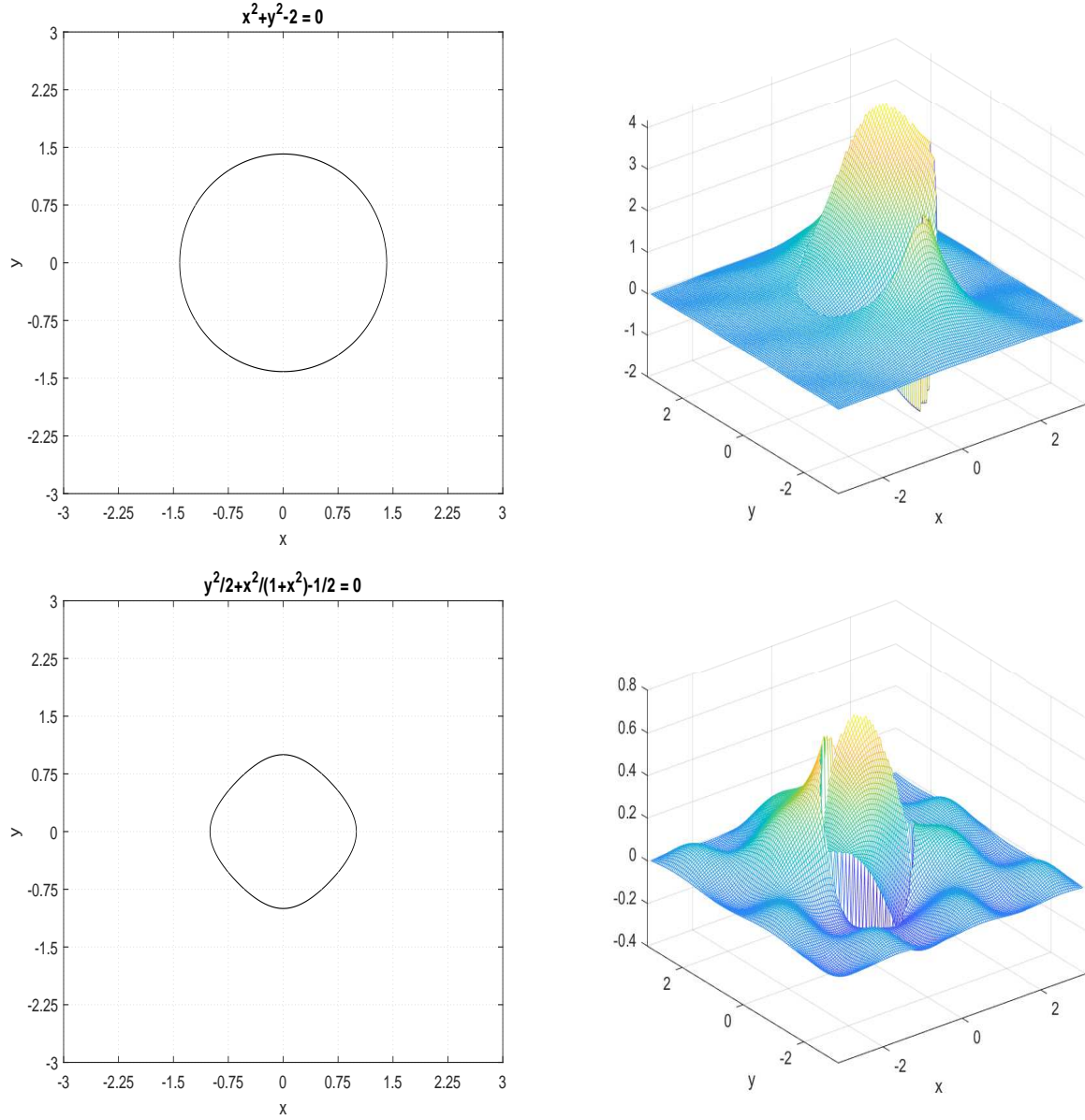


FIGURE 9. Top row for Example 5: the interface curve Γ (left) and the numerical solution u_h (right) with $h = 2^{-7} \times 2\pi$. Bottom row for Example 6: the interface curve Γ (left) and the numerical solution u_h (right) with $h = 2^{-7} \times 2\pi$.

Example 7. Let $\Omega = (-\pi, \pi)^2$ and the interface curve be given by $\Gamma := \{(x, y) \in \Omega : \psi(x, y) = 0\}$ with $\psi(x, y) = x^4 + 2y^4 - 2$. Note that $\Gamma \cap \partial\Omega = \emptyset$ and the coefficients of (1.1) are given by

$$\begin{aligned} f_+ &= f\chi_{\Omega^+} = \sin(2x)\sin(2y), & f_- &= f\chi_{\Omega^-} = \cos(2x - 2y), \\ g_0 &= 0, & g_1 &= -x^2, & g &= -y^2. \end{aligned}$$

The numerical results are provided in Table 6 and Fig. 10.

Example 8. Let $\Omega = (-\pi, \pi)^2$ and the interface curve be given by $\Gamma := \{(x, y) \in \Omega : \psi(x, y) = 0\}$ with $\psi(x, y) = y^2 - 2x^2 + x^4 - 1$. Note that $\Gamma \cap \partial\Omega = \emptyset$ and the coefficients of (1.1) are given by

$$\begin{aligned} f_+ &= f\chi_{\Omega^+} = \sin(2x)\sin(3y), & f_- &= f\chi_{\Omega^-} = \cos(2x)\sin(2y), \\ g_0 &= 0, & g_1 &= 0, & g &= -\exp(x - 2y). \end{aligned}$$

Because $g_1 = 0$, the Poisson interface problem in (1.1) simply becomes $-\nabla^2 u = f - g\delta_\Gamma$ in Ω with the Dirichlet boundary condition $u|_{\partial\Omega} = g_0$. The numerical results are provided in Table 6 and Fig. 10.

TABLE 6. Performance in Example 7 and Example 8 of the proposed sixth order compact finite difference scheme in Theorems 2.2 and 2.4 on uniform Cartesian meshes with the same mesh size $h = 2^{-J} \times 2\pi$.

J	Example 7				Example 8			
	$\frac{\ u_h - u_{h/2}\ _2}{\ u_{h/2}\ _2}$	order	$\ u_h - u_{h/2}\ _\infty$	order	$\frac{\ u_h - u_{h/2}\ _2}{\ u_{h/2}\ _2}$	order	$\ u_h - u_{h/2}\ _\infty$	order
3	5.05E+00	0	8.15E+00	0	2.88E+01	0	5.64E+02	0
4	5.56E-02	6.502	1.01E-01	6.329	4.25E-01	6.083	1.92E+01	4.878
5	1.39E-03	5.328	2.97E-03	5.092	2.41E-02	4.144	1.47E+00	3.708
6	2.78E-05	5.637	8.57E-05	5.116	1.41E-04	7.413	9.31E-03	7.300
7	1.55E-07	7.485	6.83E-07	6.971	8.88E-07	7.313	5.83E-05	7.320

Example 9. Let $\Omega = (-2, 2)^2$ and the interface curve be given by $\Gamma := \{(x, y) \in \Omega : \psi(x, y) = 0\}$ with $\psi(x, y) = 2x^4 + y^2 - 1/2$. Note that $\Gamma \cap \partial\Omega = \emptyset$ and the coefficients of (1.1) are given by

$$\begin{aligned} f_+ &= f\chi_{\Omega^+} = \sin(2\pi x) \sin(2\pi y), & f_- &= f\chi_{\Omega^-} = \sin(\pi(x + 2y)), \\ g_0 &= 0, & g_1 &= -\sin(x + y), & g &= -\sin(2x) - \sin(2y). \end{aligned}$$

The numerical results are provided in Table 7 and Fig. 11.

3.4. Numerical examples with u unknown and $\Gamma \cap \partial\Omega \neq \emptyset$. In this subsection, we provide a few numerical experiments such that the exact solution u of (1.1) is unknown and the interface curve Γ touches the boundary of Ω .

Example 10. Let $\Omega = (-\pi, \pi)^2$ and the interface curve be given by $\Gamma := \{(x, y) \in \Omega : \psi(x, y) = 0\}$ with $\psi(x, y) = y - \cos(x)$. Note that $\Gamma \cap \partial\Omega \neq \emptyset$ and the coefficients of (1.1) are given by

$$\begin{aligned} f_+ &= f\chi_{\Omega^+} = -\sin(x) \sin(3y), & f_- &= f\chi_{\Omega^-} = -\sin(2x) \sin(y), \\ g_0 &= 0, & g_1 &= 0, & g &= \sin(x). \end{aligned}$$

Because $g_1 = 0$, the Poisson interface problem in (1.1) simply becomes $-\nabla^2 u = f - g\delta_\Gamma$ in Ω with the Dirichlet boundary condition $u|_{\partial\Omega} = g_0$. The numerical results are provided in Table 7 and Fig. 11.

TABLE 7. Performance in Example 9 and Example 10 of the proposed sixth order compact finite difference scheme in Theorems 2.2 and 2.4 on uniform Cartesian meshes with the mesh sizes $h = 2^{-J} \times 4$ and $h = 2^{-J} \times 2\pi$, respectively.

J	Example 9				Example 10			
	$\frac{\ u_h - u_{h/2}\ _2}{\ u_{h/2}\ _2}$	order	$\ u_h - u_{h/2}\ _\infty$	order	$\frac{\ u_h - u_{h/2}\ _2}{\ u_{h/2}\ _2}$	order	$\ u_h - u_{h/2}\ _\infty$	order
3	6.36E+00	0	5.46E+00	0	3.21E+00	0	2.71E+00	0
4	8.46E-02	6.232	6.56E-02	6.379	2.80E-02	6.839	2.37E-02	6.840
5	7.95E-04	6.734	8.20E-04	6.322	2.01E-04	7.120	1.83E-04	7.017
6	3.86E-06	7.688	5.70E-06	7.169	1.30E-06	7.270	1.23E-06	7.211
7	7.95E-08	5.600	8.84E-08	6.011	7.62E-09	7.418	7.61E-09	7.340

Example 11. Let $\Omega = (0, 3.5)^2$ and the interface curve be given by $\Gamma := \{(x, y) \in \Omega : \psi(x, y) = 0\}$ with $\psi(x, y) = \frac{x^2}{2} + \frac{y^2}{2} - 2$. Note that $\Gamma \cap \partial\Omega \neq \emptyset$ and the coefficients of (1.1) are given by

$$\begin{aligned} f_+ &= f\chi_{\Omega^+} = \sin(\pi x) \sin(2\pi y), & f_- &= f\chi_{\Omega^-} = \sin(2\pi x) \sin(\pi y), \\ g_0 &= 0, & g_1 &= 0, & g &= -\sin(2\pi x) \sin(2\pi y). \end{aligned}$$

Because $g_1 = 0$, the Poisson interface problem in (1.1) simply becomes $-\nabla^2 u = f - g\delta_\Gamma$ in Ω with the Dirichlet boundary condition $u|_{\partial\Omega} = g_0$. The numerical results are provided in Table 8 and Fig. 12.

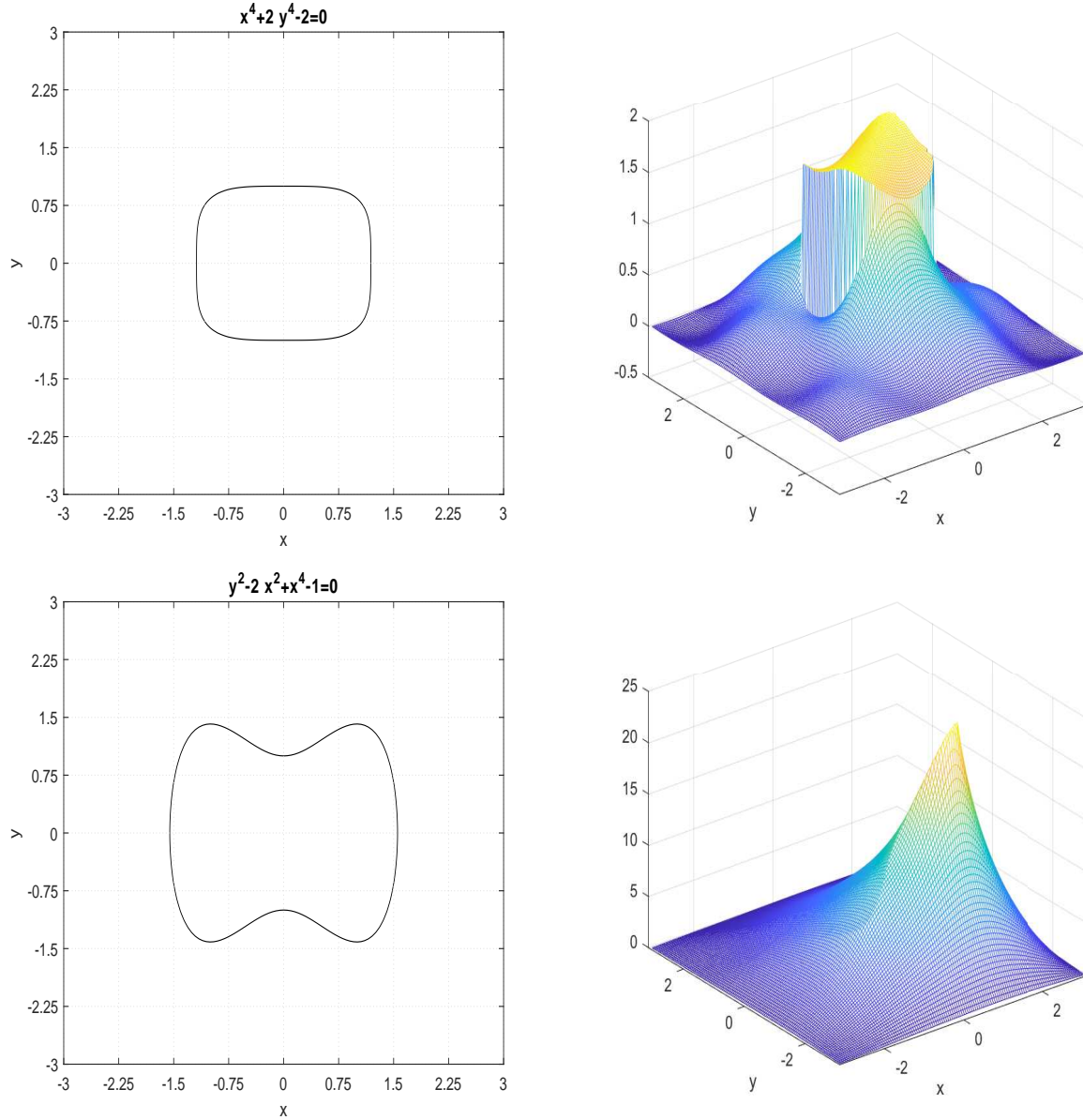


FIGURE 10. Top row for Example 7: the interface curve Γ (left) and the numerical solution u_h (right) with $h = 2^{-7} \times 2\pi$. Bottom row for Example 8: the interface curve Γ (left) and the numerical solution u_h (right) with $h = 2^{-7} \times 2\pi$.

Example 12. Let $\Omega = (-\pi, \pi)^2$ and the interface curve be given by $\Gamma := \{(x, y) \in \Omega : \psi(x, y) = 0\}$ with $\psi(x, y) = y - \sin(x)$. Note that $\Gamma \cap \partial\Omega \neq \emptyset$ and the coefficients of (1.1) are given by

$$\begin{aligned} f_+ &= f\chi_{\Omega^+} = \sin(x) \sin(3y), & f_- &= f\chi_{\Omega^-} = \sin(2x) \sin(y), \\ g_0 &= 0, & g_1 &= 0, & g &= -\sin(2x). \end{aligned}$$

Because $g_1 = 0$, the Poisson interface problem in (1.1) simply becomes $-\nabla^2 u = f - g\delta_\Gamma$ in Ω with the Dirichlet boundary condition $u|_{\partial\Omega} = g_0$. The numerical results are provided in Table 8 and Fig. 12.

Remark 3.1. For Example 12, the interface Γ is $y = \sin(x)$ which is shown in Fig. 12. Since $\Gamma \cap \partial\Omega \neq \emptyset$ and the angle between Γ and $\partial\Omega$ is not $\pi/2$, the solution will contain a singular function which will affect the convergence rate which is shown in Table 8.

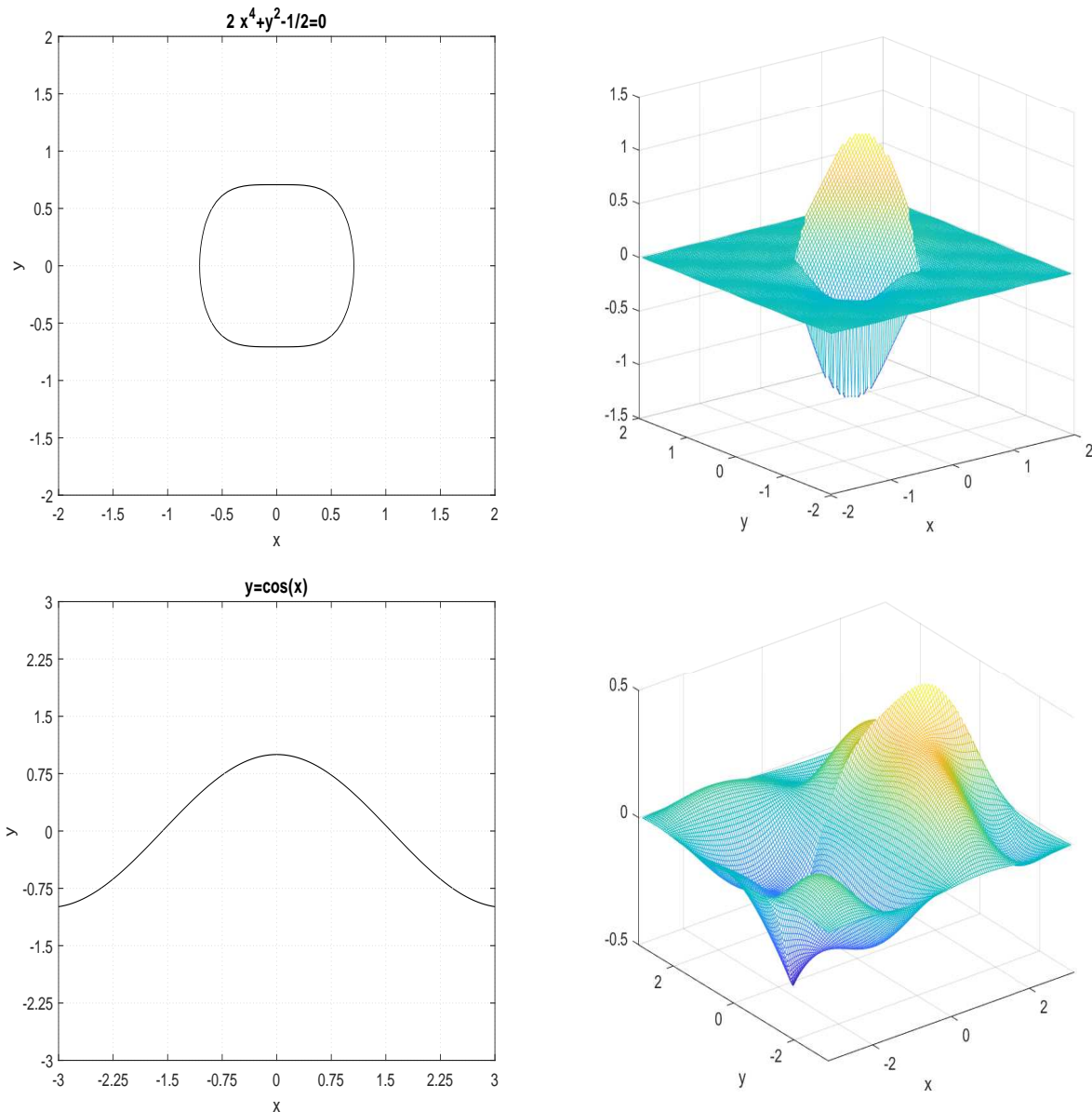


FIGURE 11. Top row for Example 9: the interface curve Γ (left) and the numerical solution u_h (right) with $h = 2^{-7} \times 4$. Bottom row for Example 10: the interface curve Γ (left) and the numerical solution u_h (right) with $h = 2^{-7} \times 2\pi$.

TABLE 8. Performance in Example 11 and Example 12 of the proposed sixth order compact finite difference scheme in Theorems 2.2 and 2.4 on uniform Cartesian meshes with $h = 2^{-J} \times 3.5$ and $h = 2^{-J} \times 2\pi$ respectively.

J	Example 11				Example 12			
	$\frac{\ u_h - u_{h/2}\ _2}{\ u_{h/2}\ _2}$	order	$\ u_h - u_{h/2}\ _\infty$	order	$\frac{\ u_h - u_{h/2}\ _2}{\ u_{h/2}\ _2}$	order	$\ u_h - u_{h/2}\ _\infty$	order
3	6.16E+00	0	3.94E-01	0	2.38E+00	0	9.54E-01	0
4	5.82E-02	6.726	4.65E-03	6.406	3.94E-03	9.236	2.36E-03	8.662
5	5.07E-04	6.844	3.43E-05	7.085	8.37E-05	5.556	8.19E-05	4.846
6	4.07E-06	6.959	3.13E-07	6.773	7.57E-06	3.468	1.57E-05	2.382
7	2.38E-07	4.098	6.00E-08	2.383	1.54E-06	2.301	6.39E-06	1.299

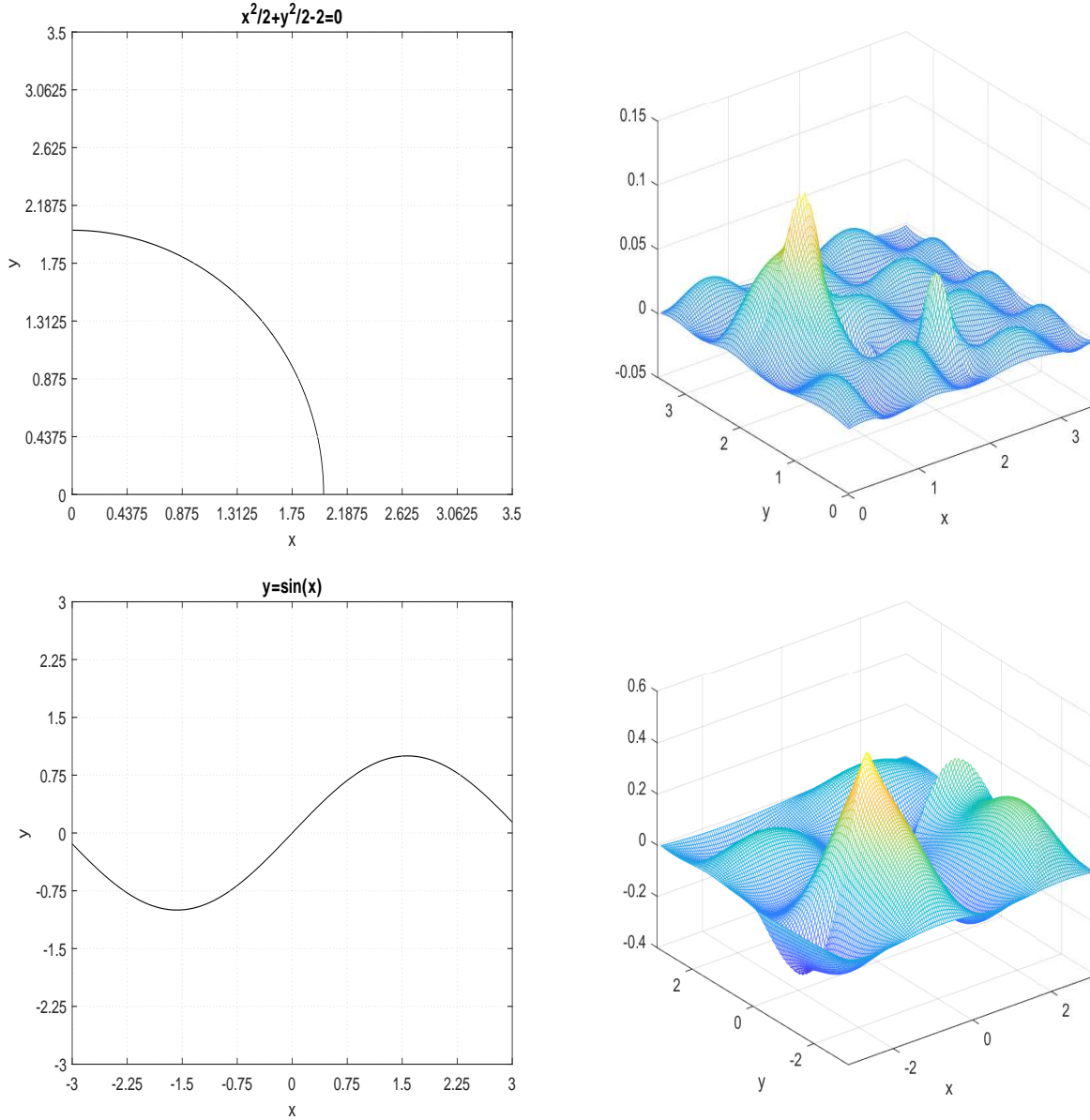


FIGURE 12. Top row for Example 11: the interface curve Γ (left) and the numerical solution u_h (right) with $h = 2^{-7} \times 3.5$. Bottom row for Example 12: the interface curve Γ (left) and the numerical solution u_h (right) with $h = 2^{-7} \times 2\pi$.

4. CONCLUSION

To our best knowledge, so far there were no compact finite difference schemes available in the literature, that can achieve fifth or sixth order for Poisson interface problems with singular source terms (1.1). Our contribution of this paper is that, we construct the sixth order compact finite difference schemes on uniform meshes for (1.1) with two non-homogeneous jump conditions and provide explicit formulas for the coefficients of the linear equations. The explicit formulas are independent on how the interface curve partitions the nine points in a stencil, so one can handle the 72 different cases configurations of the nine-point stencil with respect to the interface. The matrix A of the linear equations $Ax = b$, appearing after the discretization, is fixed for any source terms, two jump conditions and interface curves, and this allows for an easy design of preconditioners if iterative methods are used for the solution of the linear system associated with interface problems. It also allows to perform a single LU decomposition if a direct method is to be used, and solve the problem with multiple source terms/ interface conditions efficiently. This is particularly useful in case of moving

boundary problems. Our numerical experiments confirm the flexibility and the sixth order accuracy in l_2 and l_∞ norms of the proposed schemes.

APPENDIX A. PROOF OF THEOREM 2.3

Proof. Since the tangent vector at t of the curve Γ parameterized by (2.28) is given by $(x', y') = (r'(t), s'(t))$, the unit normal vector $\vec{n}(r(t) + x_i^*, s(t) + y_j^*)$ at the point $(r(t) + x_i^*, s(t) + y_j^*)$ pointing from Ω^- to Ω^+ is given by one of

$$\vec{n}(r(t) + x_i^*, s(t) + y_j^*) = \pm \frac{(y', -x')}{\sqrt{(r'(t))^2 + (s'(t))^2}} = \pm \frac{(s'(t), -r'(t))}{\sqrt{(r'(t))^2 + (s'(t))^2}}.$$

Let us firstly consider

$$\vec{n}(r(t) + x_i^*, s(t) + y_j^*) = \frac{(s'(t), -r'(t))}{\sqrt{(r'(t))^2 + (s'(t))^2}}. \quad (\text{A.1})$$

Now we shall use the interface conditions in (1.1). Plugging the parametric equation in (2.28) into the interface condition $[u] = g_1$ on Γ , near the base point (x_i^*, y_j^*) we have

$$u_+(r(t) + x_i^*, s(t) + y_j^*) - u_-(r(t) + x_i^*, s(t) + y_j^*) = g_1(r(t) + x_i^*, s(t) + y_j^*), \quad (\text{A.2})$$

for $t \in (-\epsilon, \epsilon)$. Similarly, for flux, we have

$$\begin{aligned} (\nabla u_+)(r(t) + x_i^*, s(t) + y_j^*) \cdot \vec{n}(r(t) + x_i^*, s(t) + y_j^*) - (\nabla u_-)(r(t) + x_i^*, s(t) + y_j^*) \cdot \vec{n}(r(t) + x_i^*, s(t) + y_j^*) \\ = g(r(t) + x_i^*, s(t) + y_j^*), \end{aligned}$$

for $t \in (-\epsilon, \epsilon)$. Using the unit norm vector in (A.1), the above relation becomes

$$\begin{aligned} ((\nabla u_+)(r(t) + x_i^*, s(t) + y_j^*) - (\nabla u_-)(r(t) + x_i^*, s(t) + y_j^*)) \cdot (s'(t), -r'(t)) \\ = g(r(t) + x_i^*, s(t) + y_j^*) \sqrt{(r'(t))^2 + (s'(t))^2}, \end{aligned} \quad (\text{A.3})$$

for $t \in (-\epsilon, \epsilon)$. Since all involved functions in (A.2) and (A.3) are assumed to be smooth, to link the two sets $u_+^{(m,n)}$ and $u_-^{(m,n)}$ for $(m, n) \in \Lambda_{M+1}^1$, we now take the Taylor approximation of the above functions near the base parameter $t = 0$. Using the identity in (2.25), we have

$$\begin{aligned} u_\pm(r(t) + x_i^*, s(t) + y_j^*) \\ = \sum_{(m,n) \in \Lambda_{M+1}^1} u_\pm^{(m,n)} G_{m,n}(r(t), s(t)) + \sum_{(m,n) \in \Lambda_{M-1}} f_\pm^{(m,n)} H_{m,n}(r(t), s(t)) + \mathcal{O}(t^{M+2}) \\ = \sum_{p=0}^{M+1} \left(\sum_{(m,n) \in \Lambda_{M+1}^1} u_\pm^{(m,n)} g_{m,n,p} + \sum_{(m,n) \in \Lambda_{M-1}} f_\pm^{(m,n)} h_{m,n,p} \right) t^p + \mathcal{O}(t^{M+2}), \end{aligned}$$

where the constants $g_{m,n,p}$ and $h_{m,n,p}$ only depend on $r^{(\ell)}(0)$ and $s^{(\ell)}(0)$ for $\ell = 0, \dots, M+1$, and are uniquely determined by

$$G_{m,n}(r(t), s(t)) - \sum_{p=0}^{M+1} g_{m,n,p} t^p = \mathcal{O}(t^{M+2}) \quad \text{and} \quad H_{m,n}(r(t), s(t)) - \sum_{p=0}^{M+1} h_{m,n,p} t^p = \mathcal{O}(t^{M+2}), \quad t \rightarrow 0.$$

More precisely,

$$g_{m,n,p} := \frac{1}{p!} \frac{d^p(G_{m,n}(r(t), s(t)))}{dt^p} \Big|_{t=0}, \quad h_{m,n,p} := \frac{1}{p!} \frac{d^p(H_{m,n}(r(t), s(t)))}{dt^p} \Big|_{t=0}, \quad p = 0, \dots, M+1. \quad (\text{A.4})$$

Similarly, we have

$$\begin{aligned} g_1(r(t) + x_i^*, s(t) + y_j^*) &= \sum_{(m,n) \in \Lambda_{M+1}} \frac{g_1^{(m,n)}}{m!n!} (r(t))^m (s(t))^n + \mathcal{O}(t^{M+2}) \\ &= \sum_{p=0}^{M+1} \left(\sum_{(m,n) \in \Lambda_{M+1}} \frac{g_1^{(m,n)}}{m!n!} r_{m,n,p} \right) t^p + \mathcal{O}(t^{M+2}), \end{aligned}$$

where the constants $r_{m,n,p} := \frac{1}{p!} \frac{d^p((r(t))^m(s(t))^n)}{dt^p} \Big|_{t=0}$ for $p = 0, \dots, M+1$, or equivalently,

$$(r(t))^m(s(t))^n - \sum_{p=0}^{M+1} r_{m,n,p} t^p = \mathcal{O}(t^{M+2}), \quad t \rightarrow 0.$$

Since $G_{m,n}$ is a homogeneous polynomial of degree $m+n$ and because $r(0) = s(0) = 0$, we must have $g_{m,n,p} = 0$ for all $0 \leq p < m+n$ by (A.4). Define

$$U^{(m,n)} := u_+^{(m,n)} - u_-^{(m,n)}, \quad (m,n) \in \Lambda_{M+1}^1. \quad (\text{A.5})$$

Consequently, we deduce from (A.2) that

$$\sum_{(m,n) \in \Lambda_{M+1}^1} U^{(m,n)} g_{m,n,p} = \sum_{(m,n) \in \Lambda_{M+1}^1} (u_+^{(m,n)} - u_-^{(m,n)}) g_{m,n,p} = F_p, \quad p = 0, \dots, M+1, \quad (\text{A.6})$$

where $F_0 := g_1^{(0,0)}$ and

$$F_p := \sum_{(m,n) \in \Lambda_{M-1}} (f_-^{(m,n)} - f_+^{(m,n)}) h_{m,n,p} + \sum_{(m,n) \in \Lambda_{M+1}} \frac{g_1^{(m,n)}}{m!n!} r_{m,n,p}, \quad p = 1, \dots, M+1.$$

Note that $g_{0,0,0} = 1$ and $g_{m,n,p} = 0$ for all $0 \leq p < m+n$. We observe that the identities in (A.6) can be equivalently rewritten as

$$U^{(0,0)} = F_0 = g_1^{(0,0)}, \quad (\text{A.7})$$

and

$$U^{(0,p)} g_{0,p,p} + U^{(1,p-1)} g_{1,p-1,p} = F_p - \sum_{(m,n) \in \Lambda_{M+1}^1, m+n < p} U^{(m,n)} g_{m,n,p}, \quad p = 1, \dots, M+1. \quad (\text{A.8})$$

On the other hand, we obtain from (2.25) that

$$\nabla u_{\pm}(x + x_i^*, y + y_j^*) = \sum_{(m,n) \in \Lambda_{M+1}^1} u_{\pm}^{(m,n)} \nabla G_{m,n}(x, y) + \sum_{(m,n) \in \Lambda_{M-1}} f_{\pm}^{(m,n)} \nabla H_{m,n}(x, y) + \mathcal{O}(h^{M+1}), \quad (\text{A.9})$$

for $x, y \in (-2h, 2h)$. Using (A.9) and a similar argument, we have

$$\begin{aligned} & \nabla u_{\pm}(r(t) + x_i^*, s(t) + y_j^*) \cdot (s'(t), -r'(t)) \\ &= \sum_{(m,n) \in \Lambda_{M+1}^1} u_{\pm}^{(m,n)} \nabla G_{m,n}(r(t), s(t)) \cdot (s'(t), -r'(t)) + \sum_{(m,n) \in \Lambda_{M-1}} f_{\pm}^{(m,n)} \nabla H_{m,n}(r(t), s(t)) \cdot (s'(t), -r'(t)) \\ &= \sum_{p=0}^M \left(\sum_{(m,n) \in \Lambda_{M+1}^1} u_{\pm}^{(m,n)} \tilde{g}_{m,n,p} + \sum_{(m,n) \in \Lambda_{M-1}} f_{\pm}^{(m,n)} \tilde{h}_{m,n,p} \right) t^p + \mathcal{O}(t^{M+1}), \end{aligned}$$

where the constants $\tilde{g}_{m,n,p}$ and $\tilde{h}_{m,n,p}$ are uniquely determined by

$$\begin{aligned} \nabla G_{m,n}(r(t), s(t)) \cdot (s'(t), -r'(t)) - \sum_{p=0}^M \tilde{g}_{m,n,p} t^p &= \mathcal{O}(t^{M+1}), \quad t \rightarrow 0, \\ \nabla H_{m,n}(r(t), s(t)) \cdot (s'(t), -r'(t)) - \sum_{p=0}^M \tilde{h}_{m,n,p} t^p &= \mathcal{O}(t^{M+1}), \quad t \rightarrow 0. \end{aligned}$$

More precisely, for $p = 0, \dots, M$,

$$\tilde{g}_{m,n,p} := \frac{1}{p!} \frac{d^p(\nabla G_{m,n}(r(t), s(t)) \cdot (s'(t), -r'(t)))}{dt^p} \Big|_{t=0}, \quad (\text{A.10})$$

$$\tilde{h}_{m,n,p} := \frac{1}{p!} \frac{d^p(\nabla H_{m,n}(r(t), s(t)) \cdot (s'(t), -r'(t)))}{dt^p} \Big|_{t=0}. \quad (\text{A.11})$$

Note that each entry of $\nabla G_{m,n}$ is a homogeneous polynomial of degree $m+n-1$. By $r(0) = s(0) = 0$ and (A.10), we observe that $\tilde{g}_{m,n,p} = 0$ for all $0 \leq p < m+n-1$. Similarly, we have

$$\begin{aligned} g(r(t) + x_i^*, s(t) + y_j^*) \sqrt{(r'(t))^2 + (s'(t))^2} &= \sum_{(m,n) \in \Lambda_M} \frac{g^{(m,n)}}{m!n!} (r(t))^m (s(t))^n \sqrt{(r'(t))^2 + (s'(t))^2} + \mathcal{O}(t^{M+1}) \\ &= \sum_{p=0}^M \left(\sum_{(m,n) \in \Lambda_M} \frac{g^{(m,n)}}{m!n!} \tilde{r}_{m,n,p} \right) t^p + \mathcal{O}(t^{M+1}), \end{aligned}$$

as $t \rightarrow 0$, where the constants $\tilde{r}_{m,n,p}$ for $p = 0, \dots, M$ are uniquely determined by

$$(r(t))^m (s(t))^n \sqrt{(r'(t))^2 + (s'(t))^2} - \sum_{p=0}^M \tilde{r}_{m,n,p} t^p = \mathcal{O}(t^{M+1}), \quad t \rightarrow 0.$$

Consequently, (A.3) implies that for all $p = 0, \dots, M$,

$$\sum_{(m,n) \in \Lambda_{M+1}^1} U^{(m,n)} \tilde{g}_{m,n,p} = \sum_{(m,n) \in \Lambda_{M+1}^1} \left(u_+^{(m,n)} - u_-^{(m,n)} \right) \tilde{g}_{m,n,p} = G_p, \quad p = 0, \dots, M, \quad (\text{A.12})$$

where

$$G_p := \sum_{(m,n) \in \Lambda_{M-1}} \left(f_-^{(m,n)} - f_+^{(m,n)} \right) \tilde{h}_{m,n,p} + \sum_{(m,n) \in \Lambda_M} \frac{g^{(m,n)}}{m!n!} \tilde{r}_{m,n,p}.$$

Note that $\tilde{g}_{0,0,0} = 0$ and $\tilde{g}_{m,n,p} = 0$ for all $0 \leq p < m+n-1$. We observe that the identities in (A.12) can be equivalently rewritten as

$$U^{(0,p)} \tilde{g}_{0,p,p-1} + U^{(1,p-1)} \tilde{g}_{1,p-1,p-1} = G_{p-1} - \sum_{(m,n) \in \Lambda_{M+1}^1, m+n < p} U^{(m,n)} \tilde{g}_{m,n,p-1}, \quad p = 1, \dots, M+1. \quad (\text{A.13})$$

Using our assumption $(r'(0))^2 + (s'(0))^2 > 0$ in (2.28), we now claim that

$$g_{0,p,p} \tilde{g}_{1,p-1,p-1} - g_{1,p-1,p} \tilde{g}_{0,p,p-1} > 0, \quad \forall p = 1, \dots, M. \quad (\text{A.14})$$

Since the polynomial $G_{m,n}$ in (2.9) is a homogeneous polynomial of degree $m+n$, we observe

$$g_{m,n,m+n} = G_{m,n}(r'(0), s'(0)), \quad (m,n) \in \Lambda_{M+1}^1. \quad (\text{A.15})$$

From the definition of $G_{m,n}(x, y)$ in (2.9), we particularly have

$$g_{0,p,p} = \sum_{\ell=0}^{\lfloor \frac{p}{2} \rfloor} (-1)^\ell \frac{(r'(0))^{2\ell} (s'(0))^{p-2\ell}}{(2\ell)!(p-2\ell)!} \quad \text{and} \quad g_{1,p-1,p} = \sum_{\ell=0}^{\lfloor \frac{p-1}{2} \rfloor} (-1)^\ell \frac{(r'(0))^{1+2\ell} (s'(0))^{p-1-2\ell}}{(1+2\ell)!(p-1-2\ell)!}. \quad (\text{A.16})$$

Clearly,

$$\left\lfloor \frac{p}{2} \right\rfloor = \begin{cases} \lfloor \frac{p-1}{2} \rfloor + 1, & \text{if } p \text{ is even,} \\ \lfloor \frac{p-1}{2} \rfloor, & \text{if } p \text{ is odd,} \end{cases} \quad \text{and} \quad 2 \left\lfloor \frac{p-1}{2} \right\rfloor + 1 = p, \quad \text{if } p \text{ is odd.} \quad (\text{A.17})$$

Similarly, we also have

$$\tilde{g}_{m,n,m+n-1} = \nabla G_{m,n}(r'(0), s'(0)) \cdot (s'(0), -r'(0)), \quad (m,n) \in \Lambda_{M+1}^1. \quad (\text{A.18})$$

From the definition of $G_{m,n}(x, y)$ in (2.9), we deduce that

$$\begin{aligned} \tilde{g}_{0,p,p-1} &= \nabla G_{0,p}(r'(0), s'(0)) \cdot (s'(0), -r'(0)) \\ &= \sum_{\ell=1}^{\lfloor \frac{p}{2} \rfloor} (-1)^\ell \frac{(r'(0))^{2\ell-1} (s'(0))^{p+1-2\ell}}{(2\ell-1)!(p-2\ell)!} - \sum_{\ell=0}^{\lfloor \frac{p-1}{2} \rfloor} (-1)^\ell \frac{(r'(0))^{2\ell+1} (s'(0))^{p-2\ell-1}}{(2\ell)!(p-2\ell-1)!} \\ &= - \sum_{\ell=0}^{\lfloor \frac{p}{2} \rfloor - 1} (-1)^\ell \frac{(r'(0))^{2\ell+1} (s'(0))^{p-2\ell-1}}{(2\ell+1)!(p-2\ell-2)!} - \sum_{\ell=0}^{\lfloor \frac{p-1}{2} \rfloor} (-1)^\ell \frac{(r'(0))^{2\ell+1} (s'(0))^{p-2\ell-1}}{(2\ell)!(p-2\ell-1)!}. \end{aligned} \quad (\text{A.19})$$

By (A.16), (A.17) and (A.19), we conclude that

$$\tilde{g}_{0,p,p-1} = -p \sum_{\ell=0}^{\lfloor \frac{p-1}{2} \rfloor} (-1)^\ell \frac{(r'(0))^{2\ell+1} (s'(0))^{p-2\ell-1}}{(2\ell+1)!(p-2\ell-1)!} = -pg_{1,p-1,p}. \quad (\text{A.20})$$

Similarly,

$$\begin{aligned} \tilde{g}_{1,p-1,p-1} &= \nabla G_{1,p-1}(r'(0), s'(0)) \cdot (s'(0), -r'(0)) \\ &= \sum_{\ell=0}^{\lfloor \frac{p-1}{2} \rfloor} (-1)^\ell \frac{(r'(0))^{2\ell} (s'(0))^{p-2\ell}}{(2\ell)!(p-1-2\ell)!} - \sum_{\ell=0}^{\lfloor \frac{p}{2} \rfloor - 1} (-1)^\ell \frac{(r'(0))^{2\ell+2} (s'(0))^{p-2\ell-2}}{(2\ell+1)!(p-2\ell-2)!} \\ &= \sum_{\ell=0}^{\lfloor \frac{p-1}{2} \rfloor} (-1)^\ell \frac{(r'(0))^{2\ell} (s'(0))^{p-2\ell}}{(2\ell)!(p-1-2\ell)!} + \sum_{\ell=1}^{\lfloor \frac{p}{2} \rfloor} (-1)^\ell \frac{(r'(0))^{2\ell} (s'(0))^{p-2\ell}}{(2\ell-1)!(p-2\ell)!}. \end{aligned} \quad (\text{A.21})$$

By (A.16), (A.17) and (A.21), we deduce that

$$\tilde{g}_{1,p-1,p-1} = p \sum_{\ell=0}^{\lfloor \frac{p}{2} \rfloor} (-1)^\ell \frac{(r'(0))^{2\ell} (s'(0))^{p-2\ell}}{(2\ell)!(p-2\ell)!} = pg_{0,p,p}. \quad (\text{A.22})$$

By (A.20) and (A.22),

$$g_{0,p,p} \tilde{g}_{1,p-1,p-1} - g_{1,p-1,p} \tilde{g}_{0,p,p-1} = p(g_{0,p,p})^2 + p(g_{1,p-1,p})^2, \quad \forall p = 1, \dots, M+1. \quad (\text{A.23})$$

Let

$$W := (p!)^2 (g_{0,p,p})^2 + (p!)^2 (g_{1,p-1,p})^2, \quad a := (r'(0))^2 \quad \text{and} \quad b := (s'(0))^2. \quad (\text{A.24})$$

Then

$$\begin{aligned} W &= \left(\sum_{\ell=0}^{\lfloor \frac{p}{2} \rfloor} (-1)^\ell \binom{p}{2\ell} a^\ell b^{p/2-\ell} \right)^2 + \left(\sum_{\ell=0}^{\lfloor \frac{p-1}{2} \rfloor} (-1)^\ell \binom{p}{2\ell+1} a^{1/2+\ell} b^{(p-1)/2-\ell} \right)^2 \\ &= \sum_{i=0}^{\lfloor \frac{p}{2} \rfloor} \sum_{j=0}^{\lfloor \frac{p}{2} \rfloor} (-1)^{i+j} \binom{p}{2i} \binom{p}{2j} a^{i+j} b^{p-i-j} + \sum_{i=0}^{\lfloor \frac{p-1}{2} \rfloor} \sum_{j=0}^{\lfloor \frac{p-1}{2} \rfloor} (-1)^{i+j} \binom{p}{2i+1} \binom{p}{2j+1} a^{1+i+j} b^{p-1-i-j} \\ &= \sum_{\ell=0}^{2\lfloor \frac{p}{2} \rfloor} \sum_{i=\max(0, \ell-\lfloor \frac{p}{2} \rfloor)}^{\min(\ell, \lfloor \frac{p}{2} \rfloor)} (-1)^\ell \binom{p}{2i} \binom{p}{2(\ell-i)} a^\ell b^{p-\ell} \\ &\quad - \sum_{\ell=0}^{2\lfloor \frac{p-1}{2} \rfloor + 1} \sum_{i=\max(0, \ell-\lfloor \frac{p+1}{2} \rfloor)}^{\min(\ell-1, \lfloor \frac{p-1}{2} \rfloor)} (-1)^\ell \binom{p}{2i+1} \binom{p}{2(\ell-i)-1} a^\ell b^{p-\ell}. \end{aligned} \quad (\text{A.25})$$

Let us consider the first case: p is even and $\ell \leq \lfloor \frac{p}{2} \rfloor$. Then

$$\begin{aligned} &\sum_{i=\max(0, \ell-\lfloor \frac{p}{2} \rfloor)}^{\min(\ell, \lfloor \frac{p}{2} \rfloor)} (-1)^\ell \binom{p}{2i} \binom{p}{2(\ell-i)} - \sum_{i=\max(0, \ell-\lfloor \frac{p+1}{2} \rfloor)}^{\min(\ell-1, \lfloor \frac{p-1}{2} \rfloor)} (-1)^\ell \binom{p}{2i+1} \binom{p}{2(\ell-i)-1} \\ &= \sum_{i=0}^{\ell} (-1)^\ell \binom{p}{2i} \binom{p}{2(\ell-i)} - \sum_{i=0}^{\ell-1} (-1)^\ell \binom{p}{2i+1} \binom{p}{2(\ell-i)-1} \\ &= (-1)^\ell \sum_{i=0,2,4}^{2\ell} \binom{p}{i} \binom{p}{2\ell-i} - (-1)^\ell \sum_{i=1,3,5}^{2\ell-1} \binom{p}{i} \binom{p}{2\ell-i} = (-1)^\ell \sum_{i=0}^{2\ell} (-1)^i \binom{p}{i} \binom{p}{2\ell-i} \\ &= (-1)^\ell \sum_{i=0}^{2\ell} \text{coeff}((1-x)^p, x^i) \text{coeff}((1+x)^p, x^{2\ell-i}) = (-1)^\ell \text{coeff}((1-x^2)^p, x^{2\ell}) = \binom{p}{\ell}, \end{aligned} \quad (\text{A.26})$$

where the $\text{coeff}(f(x), x^n)$ function extracts the coefficient of x^n in the polynomial $f(x)$. Similarly, we can prove that other cases can obtain the same result. By (A.24), (A.25) and (A.26),

$$W = \sum_{\ell=0}^p \binom{p}{\ell} a^\ell b^{p-\ell} = (a+b)^p = \left((r'(0))^2 + (s'(0))^2 \right)^p. \quad (\text{A.27})$$

According to (A.23), (A.24), (A.27) and (2.28),

$$g_{0,p,p} \tilde{g}_{1,p-1,p-1} - g_{1,p-1,p} \tilde{g}_{0,p,p-1} > 0, \quad \forall p = 1, \dots, M+1. \quad (\text{A.28})$$

Consequently, the associated 2×2 coefficient matrix in the linear system in (A.8) and (A.13) is invertible and its inverse is given by

$$Q_p := \frac{1}{g_{0,p,p} \tilde{g}_{1,p-1,p-1} - g_{1,p-1,p} \tilde{g}_{0,p,p-1}} \begin{bmatrix} \tilde{g}_{1,p-1,p-1} & -g_{1,p-1,p} \\ -\tilde{g}_{0,p,p-1} & g_{0,p,p} \end{bmatrix}.$$

Hence, the linear equations in (A.8) and (A.13) must have a unique solution $\{U^{(0,p)}, U^{(1,p-1)}\}_{p=1, \dots, M}$, which can be recursively computed from $p=1$ to $p=M$ by $U^{(0,0)} = g_1^{(0,0)}$ due to (A.7) and

$$\begin{bmatrix} U^{(0,p)} \\ U^{(1,p-1)} \end{bmatrix} = Q_p \begin{bmatrix} F_p \\ G_{p-1} \end{bmatrix} - \sum_{n=1}^{p-1} Q_p \begin{bmatrix} U^{(0,n)} g_{0,n,p} + U^{(1,n-1)} g_{1,n-1,p} \\ U^{(0,n)} \tilde{g}_{0,n,p-1} + U^{(1,n-1)} \tilde{g}_{1,n-1,p-1} \end{bmatrix}, \quad p = 1, \dots, M+1. \quad (\text{A.29})$$

Note that for $p=1$, the above summation $\sum_{n=1}^{p-1}$ is empty.

If the normal vector \vec{n} in (A.1) gives the direction from Ω^+ to Ω^- , then we only need to add a negative sign to all $\tilde{r}_{m,n,p}$. Since $U^{(m,n)} = u_+^{(m,n)} - u_-^{(m,n)}$, the identities in (A.29) and (A.7) prove all the claims. \square

REFERENCES

- [1] I. Babuška, B. Andersson, B. Guo, J. M. Melenk and H. S. Oh, Finite element method for solving problems with singular solutions. *J. Comput. Appl. Math.* **74** (1996), no. 1-2, 51-70.
- [2] M. Blumenfeld, The regularity of interface-problems on corner-regions. *Lecture Notes in Math.* **1121** (1985), 38-54.
- [3] G. Brandstetter and S. Govindjee, A high-order immersed boundary discontinuous-Galerkin method for Poisson's equation with discontinuous coefficients and singular sources. *Int. J. Numer. Meth. Engng.* **101** (2015), no. 11, 847-869.
- [4] Z. Cai and S. Kim, A finite element method using singular functions for the Poisson equation: corner singularities. *SIAM J. Numer. Anal.* **39** (2001), no. 1, 286-299.
- [5] J. M. Chadam and H. M. Yin, A diffusion equation with localized chemical reactions. *Proc. Edinburgh Math. Soc.* **37** (1993), 101-118.
- [6] X. Chen, X. Feng and Z. Li, A direct method for accurate solution and gradient computations for elliptic interface problems. *Numer. Algorithms.* **80** (2019), 709-740.
- [7] B. Dong, X. Feng and Z. Li, An FE-FD method for anisotropic elliptic interface problems. *SIAM J. Sci. Comput.* **42** (2020), no. 4, B1041-B1066.
- [8] R. Egan and F. Gibou, Geometric discretization of the multidimensional Dirac delta distribution-Application to the Poisson equation with singular source terms. *J. Comput. Phys.* **346** (2017), 71-90.
- [9] A. Ern and J.-L. Guermond, Theory and practice of finite elements. *Vol. 159. Springer Science & Business Media*, 2013.
- [10] X. Feng, Z. Li and Z. Qiao, High order compact finite difference schemes for the Helmholtz equation with discontinuous coefficients. *J. Comput. Math.* **29** (2011), no. 3, 324-340.
- [11] G. J. Fix, S. Gulati and G. I. Wakoff, On the use of singular functions with finite element approximations. *J. Comput. Phys.* **13** (1973), 209-228.
- [12] B. Guo and H. S. Oh, The h-p version of the finite element method for problems with interfaces. *Int. J. Numer. Methods. Eng.* **37** (1994), no. 10, 1741-1762.
- [13] T. Y. Hou and X. Wu, A multiscale finite element method for elliptic problems in composite materials and porous media. *J. Comput. Phys.* **134** (1997), 169-189.
- [14] H. Ji, J. Chen and Z. Li, A high-order source removal finite element method for a class of elliptic interface problems. *Appl. Numer. Math.* **130** (2018), 112-130.
- [15] J. D. Kandilarov and L. G. Vulkov, The immersed interface method for two-dimensional heat-diffusion equations with singular own sources. *Appl. Numer. Math.* **57** (2007), no. 5-7, 486-497.
- [16] R. B. Kellogg, Singularities in interface problems. *Numerical Solution of Partial Differential Equations-II* (1971), 351-400.
- [17] R. B. Kellogg, On the Poisson equation with intersecting interfaces. *Appl. Anal.* **4** (1975), no. 2, 101-129.

- [18] R. B. Kellogg, Higher order singularities for interface problems. *The Mathematical Foundations of the Finite Element Method with Applications to Partial Differential Equations* (1972), 589-602.
- [19] S. Kim, Z. Cai, J. Pyo and S. Kong, A finite element method using singular functions: interface problems. *Hokkaido Math. J.* **36** (2007), no. 4, 815-836.
- [20] S. Kim and S. Kong, A finite element method dealing the singular points with a cut-off function. *J. Appl. Math. Comput.* **21** (2006), no. 1-2, 141-152.
- [21] R. J. Leveque and Z. Li, The Immersed interface method for elliptic equations with discontinuous coefficients and singular sources. *SIAM J. Numer. Anal.* **31** (1994), no. 4, 1019-1044.
- [22] R. J. Leveque and Z. Li, Immersed interface methods for stokes flow with elastic boundaries or surface tension. *SIAM J. Sci. Comput.* **18** (1997), no. 3, 709-735.
- [23] Z. Li and K. Ito, The immersed interface method: numerical solutions of PDEs involving interfaces and irregular domains. *Society for Industrial and Applied Mathematics*. 2006.
- [24] Z. Li, A fast iterative algorithm for elliptic interface problems. *SIAM J. Numer. Anal.* **35** (1998), no. 1, 230-254.
- [25] Z. Li, A note on immersed interface method for three-dimensional elliptic equations. *Comput. Math. with Appl.* **31** (1996), no. 3, 9-17.
- [26] S. Nicaise, Polygonal interface problems: higher regularity results. *Commun. Partial. Differ. Equ.* **15** (1990), no. 10, 1475-1508.
- [27] S. Nicaise and A. M. Sandig, General interface problems-I. *Math. Methods Appl. Sci.* **17** (1994), 395-429.
- [28] M. Petzoldt, Regularity results for Laplace interface problems in two dimensions. *J. Anal. Appl.* **20** (2001), no. 2, 431-455.
- [29] M. Petzoldt, A posteriori error estimators for elliptic equations with discontinuous coefficients. *Adv. Comput. Math.* **16** (2002), no. 1, 47-75.
- [30] D. A. D. Pietro and A. Ern, Mathematical aspects of discontinuous Galerkin methods. *Springer Science and Business Media*. 2011.
- [31] A. A. Samarskii, V. L. Makarov, and R. D. Lazarov, Difference schemes for differential equations with generalized solutions, Vysshaya Shkola, (Russian), Moscow (1987)
- [32] S. O. Settle, C. C. Douglas, I. Kim, and D. Sheen, On the derivation of highest-order compact finite difference schemes for the one- and two-dimensional Poisson equation with Dirichlet boundary conditions. *SIAM J. Numer. Anal.* **51** (2013), no. 4, 2470-2490.
- [33] A. K. Tornberg and B. Engquist, Numerical approximations of singular source terms in differential equations. *J. Comput. Phys.* **200** (2004), no. 2, 462-488.
- [34] J. D. Towers, Finite difference methods for discretizing singular source terms in a Poisson interface problem. *Contemp. Math.* **526** (2010), 359-389.
- [35] J. L. Vazquez, The Porous medium equation: mathematical theory. *Clarendon Press*. 2007. p15.
- [36] Y. Wang and J. Zhang, Sixth order compact scheme combined with multigrid method and extrapolation technique for 2D Poisson equation. *J. Comput. Phys.* **228** (2009), no. 1, 137-146.
- [37] A. Wiegmann and K. P. Bube, The explicit-jump immersed interface method: finite difference methods for PDEs with piecewise smooth solutions. *SIAM J. Numer. Anal.* **37** (2000), no. 3, 827-862.
- [38] S. Zhai, X. Feng and Y. He, A family of fourth-order and sixth-order compact difference schemes for the three-dimensional Poisson equation. *J. Sci. Comput.* **54** (2013), 97-120.
- [39] Y. C. Zhou, S. Zhao, M. Feig and G. W. Wei, High order matched interface and boundary method for elliptic equations with discontinuous coefficients and singular sources. *J. Comput. Phys.* **213** (2006), no. 1, 1-30.
- [40] C. S. Peskin, The immersed boundary method. *Acta Numerica* (2002), 479-517.